Human blood metabolite timetable indicates internal body time

Takeya Kasukawa[a,1], Masahiro Sugimoto[b,c,1], Akiko Hida[d], Yoichi Minami[e], Masayo Mori[b], Sato Honma[f], Ken-ichi Honma[f], Kazuo Mishima[d], Tomoyoshi Soga[b,2], and Hiroki R. Ueda[a,e,g,h,i,2]

[a]Functional Genomics Unit, and [e]Laboratory for Systems Biology, RIKEN Center for Developmental Biology, Chuo-ku, Kobe, Hyogo 650-0047, Japan; [b]Institute for Advanced Biosciences, Keio University, Tsuruoka, Yamagata 997-0017, Japan; [c]Laboratory for Malignancy Control Research, Medical Innovation Center, Graduate School of Medicine and Faculty of Medicine, Kyoto University, Yoshida-Konoe, Sakyo-ku, Kyoto 606-8501, Japan; [d]Department of Psychophysiology, National Institute of Mental Health, National Center of Neurology and Psychiatry, Kodaira, Tokyo 187-8553, Japan; [f]Department of Chronomedicine, Hokkaido University Graduate School of Medicine, Kita-ku, Sapporo 060-8638, Japan; [g]Department of Biological Sciences, Graduate School of Science, Osaka University, Toyonaka, Osaka 560-0043, Japan; [h]Department of Mathematics, Graduate School of Science, Kyoto University, Kitashirakawa Oiwake-cho, Sakyo-ku, Kyoto 606-8502, Japan; and [i]Laboratory for Synthetic Biology, RIKEN Quantitative Biology Center, Chuo-ku, Kobe, Hyogo 650-0047, Japan

Edited by Joseph S. Takahashi, Howard Hughes Medical Institute, University of Texas Southwestern Medical Center, Dallas, TX, and approved July 20, 2012 (received for review May 8, 2012)

A convenient way to estimate internal body time (BT) is essential for chronotherapy and time-restricted feeding, both of which use body-time information to maximize potency and minimize toxicity during drug administration and feeding, respectively. Previously, we proposed a molecular timetable based on circadian-oscillating substances in multiple mouse organs or blood to estimate internal body time from samples taken at only a few time points. Here we applied this molecular-timetable concept to estimate and evaluate internal body time in humans. We constructed a 1.5-d reference timetable of oscillating metabolites in human blood samples with 2-h sampling frequency while simultaneously controlling for the confounding effects of activity level, light, temperature, sleep, and food intake. By using this metabolite timetable as a reference, we accurately determined internal body time within 3 h from just two anti-phase blood samples. Our minimally invasive, molecular-timetable method with human blood enables highly optimized and personalized medicine.

metabolomics | circadian rhythm | liquid chromatography mass spectrometry | diagnostic tool

Many organisms possess a molecular time-keeping mechanism, a circadian clock, which has endogenous, self-sustained oscillations with a period of about 24 h. Circadian regulation of cell activity occurs in diverse biological processes such as electrical activity, gene/protein expression, and concentration of ions and substances (1, 2). In mammals, for example, several clock genes regulate circadian gene expression in central and peripheral clock tissues (3–9), as well as metabolites in the blood (10–15). Reflecting circadian regulation of such processes, the potency and toxicity of administered drugs depends on an individual's body time (BT) (16–22). Drug delivery according to body time improves the outcome of pharmacotherapy by maximizing potency and minimizing toxicity (23), and administrating drugs at an inappropriate body time can result in severe side effects (22). For example, rhythm disturbances were induced by administration of IFN-α during the early active phase in mice, although unaffected during the early rest phase (22); and the time of administration of two anticancer drugs, adriamycin (6:00 AM) and cisplatin (6:00 PM), made a lower toxicity effect than its antiphasic administration (24). However, several reports showed that internal body time varies by 5–6 h in healthy humans (25, 26) and as much as 10–12 h in shift workers without forced entrainments (27, 28). Therefore, for efficient application of body-time drug delivery or "chronotherapy" (16–20) in a clinical setting, a simple and robust method for estimating an individual's internal body time is needed.

Additionally, the timing of food intake may contribute to weight gain (29) and metabolic disease (30) because energy regulation and circadian rhythms are molecularly and physiologically intertwined (31–41). For example, mice fed a high-fat diet during a 12-h light phase gain significantly more weight than mice fed only during a 12-h dark phase (29). These results suggest that food intake at different body times can alleviate or exacerbate diet-induced obesity. Therefore, an accurate and convenient way to detect internal body time may improve time-restricted diet strategies.

One conventional way to estimate human internal body time is to periodically sample for more than 24 h the level of melatonin or cortisol, which have robust circadian oscillations in the blood (10–12). Although this strategy directly measures internal body time, it requires labor-intensive constant sampling under controlled environmental conditions to reveal metabolite peaks and rhythms. To reduce this burden, we previously developed a molecular-timetable method (12, 42), which was inspired by Linné's flower clock (Fig. 1*A*). In Linné's flower clock, one can estimate the time of day by watching the opening and closing pattern of various flowers. Similarly, by using our molecular timetable method, one can estimate the body time of day by profiling the circadian oscillation patterns of gene expression or metabolites in the body. Compared with the conventional method, the molecular-timetable method requires only one or few time-point samplings. In mice, this method works with the expression activity of clock-controlled genes in different organs (42, 43) and with oscillatory metabolites in blood plasma (12).

In this study, we applied this method to detect internal body time using blood samples in humans (Fig. 1*B*). First, we used liquid chromatography mass spectrometry (LC–MS) (44–46) to measure the abundance of various metabolites in blood plasma samples from several healthy human subjects over 1.5 d while controlling for activity level, environmental changes, sleep, and food intake. From these data we constructed a molecular timetable of metabolites that oscillate over 24-h, arranged according to their peak abundance during the day. This reference metabolite timetable enabled us to accurately detect an individual's body time with only two samples of blood drawn 12 h apart. Our study demonstrates that human internal body time can be detected using limited time-point sampling and a reference metabolite timetable.

Author contributions: T.K., M.S., A.H., Y.M., M.M., S.H., K.H., K.M., T.S., and H.R.U. designed research; T.K., M.S., A.H., Y.M., M.M., S.H., K.M., and H.R.U. performed research; M.S. contributed new reagents/analytic tools; T.K., M.S., A.H., Y.M., and M.M. analyzed data; and T.K., M.S., A.H., M.M., and H.R.U. wrote the paper.

The authors declare no conflict of interest.

This article is a PNAS Direct Submission.

Freely available online through the PNAS open access option.

[1]T.K. and M.S. contributed equally to this work.

[2]To whom correspondence may be addressed. E-mail: uedah-tky@umin.ac.jp or soga@sfc.keio.ac.jp.

This article contains supporting information online at www.pnas.org/lookup/suppl/doi:10.1073/pnas.1207768109/-/DCSupplemental.

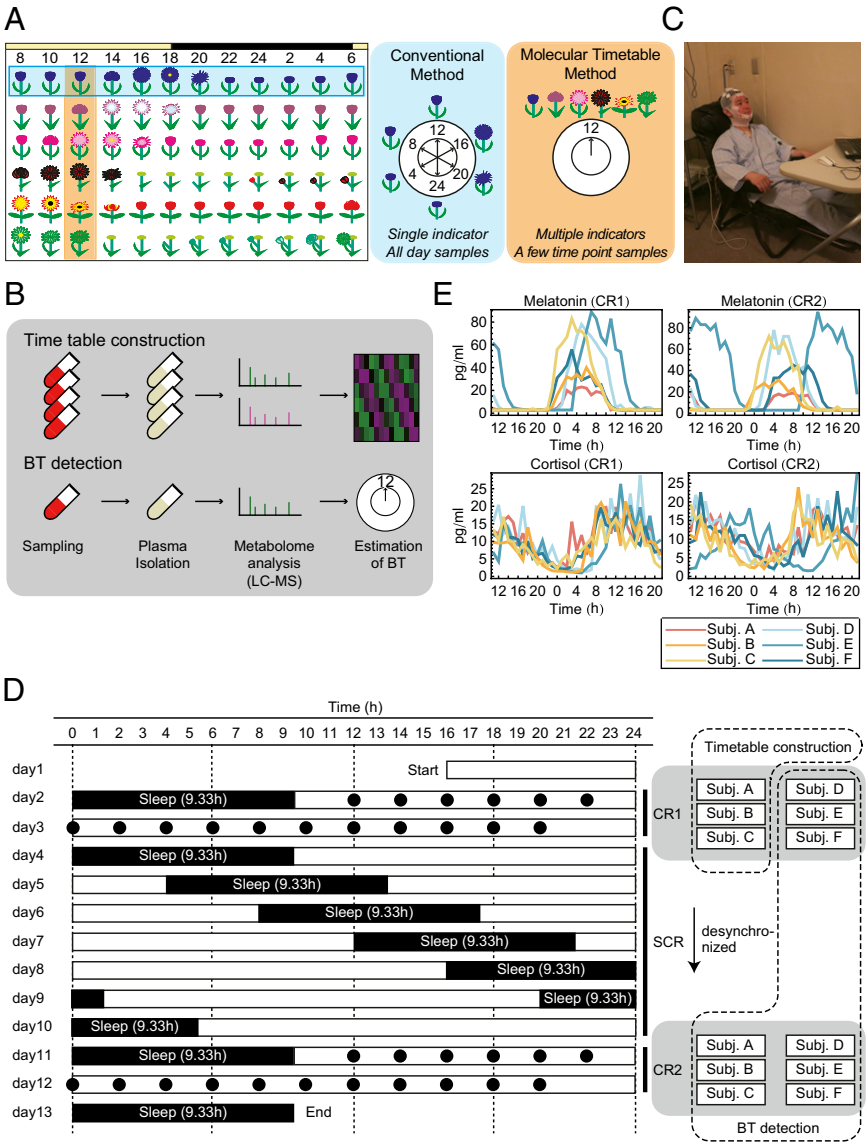

Fig. 1. Experimental condition. (*A*) The concept of body-time detection with conventional and molecular timetable methods illustrated by Linné's flower clock. In the conventional method a single indicator monitored over a few days detects internal body time; in the molecular timetable method, multiple metabolic "flowers" are simultaneously measured at a few time points, which reduce efforts in sampling. (*B*) Metabolite timetable construction. We collected time-course blood samples, isolated plasma, measured with LC–MS, and selected circadian-oscillating metabolites as indicators. In body-time detection, we collected blood samples at a few time points, isolated plasma, measured with LC–MS, and estimated body time. (*C*) Image of the constant routine (CR) experiments. During CR, subjects stayed in chairs while various measurements were performed. Note: the man in this picture is demonstrating the set-up and is not an actual subject in this study. (*D*) Sampling schedule for each subject. Black circles indicate the time points when blood samples were taken and when subjects ate during CR. White boxes indicate the time when subjects were awake, and black boxes indicate when they were asleep. The blood samples of three subjects during CR1 were used for timetable construction, and other samples were used for body-time estimation. (*E*) Measured melatonin (*Upper*) and cortisol (*Lower*) rhythms in the collected blood samples during CR1 (*Left*) and CR2 (*Right*). The cortisol and melatonin levels show that some subjects (e.g., subject E in CR2) have shifted internal body time against sampled time. CR, constant routine; SCR, semiconstant routine; BT, body time; LC–MS, liquid chromatography mass spectrometry.

Results

Construction of Human Blood Molecular Timetable. First, we aimed to construct a molecular timetable that includes a list of oscillating metabolites in human blood with information on mean, amplitude, and peak time (PT) of metabolite abundance over 24 h. We recruited six healthy volunteers (subjects A–F) who stayed in an environmentally controlled sleep laboratory for about 2 wk and underwent a forced desynchronization (FD) protocol consisting of three activity routines—constant routine one (CR1), then semiconstant routine (SCR), and finally constant routine two (CR2) (Fig. 1 *C* and *D*). The FD protocol used in this study was composed of the following three parts: (*i*) measurement under CR1 (47) followed by (*ii*) a 28-h sleep–wake schedule for 7 d during SCR (48), and (*iii*) a second measurement under CR2. The 28-h sleep–wake schedule enforces desynchronization between sleep homeostasis and circadian cycle. Therefore, the circadian clock of each individual runs according to his/her own period length and hence reveals the variability of its natural frequency or phase during CR2 after SCR.

Blood samples were collected every hour for 1.5 d in CR1 and CR2 with a defined caloric amount of food eaten every 2 h. We measured the time-course abundance of melatonin and cortisol in these blood plasma samples by RIA and found a wide variation in melatonin and cortisol rhythms (Fig. 1*E*). We used blood samples from three subjects (subjects A–C) in CR1 to construct a standard metabolic timetable because their body time most closely matched each other and previously reported melatonin and cortisol rhythms. We note that constructing a timetable with any combination of subjects did not change the results of our study (*SI Results and Discussion*).

We used an LC–MS system to obtain the abundance of various metabolites for each subject at 17 time points (every 2 h) in each constant routine (CR1 or CR2) for a total of 204 samples. Using the three blood sample sets of CR1 from subjects A–C (51 samples in total) for molecular timetable construction, 2,541 and 1,796 metabolite peaks were detected in the positive and negative ion modes, respectively. To select circadian-oscillating metabolite peaks from these, we performed cosine fitting to the mean peak area of each sample set, which is averaged over three individuals at the same time point, and tested the significance of circadian rhythmicity by permutation tests (i.e., calculating the probability by using randomly shuffled time-course data of mean peak area). With the cutoff false discovery rate (FDR; the expected proportions of false positives in the selected set) of ≤0.1,

we obtained 142 and 168 metabolite peaks of positive and negative ions, respectively, as circadian-oscillating metabolite peaks. These peaks include circadian-oscillating metabolite peaks with larger or smaller amplitudes and, as a result, some of them show variability among the three individuals. This is because our initial test only selects for peaks with significant circadian rhythmicity, but not significant amplitude. Thus, we further selected circadian-oscillating metabolite peaks with significant amplitude, whose circadian amplitude was significantly larger than the variations among individuals, with the cutoff FDR of ≤0.1 in a one-way ANOVA analysis. Consequently, the substantial overall cutoff is $0.1 \times 0.1 = 0.01$ because metabolite peaks were filtered by two independent criteria (FDR ≤ 0.1), and this is equivalent to FDR ≤ 0.01 used in our previous mouse study (12). As a final set of circadian-oscillating metabolites (with significant rhythmicity and amplitude), we obtained 33 and 25 metabolite peaks of positive and negative ions, respectively (Fig. 2 and Dataset S1). The procedure for the molecular timetable construction is illustrated in Fig. S1. The number of metabolite peaks (58 peaks) is adequate for body-time estimation because we previously found that 20 metabolites were sufficient for accurate body-time estimation (12).

Body-Time Estimation with Metabolic Molecular Timetable. We analyzed the remaining nine blood sample sets (three sample sets from subjects D–F in CR1 and all six sample sets from subjects A–F in CR2) to test the accuracy of our molecular timetable method. To evaluate its accuracy, we determined the "expected body time" for each sample set by a conventional method (Fig. 1*A*) using cosine fitting to time-course data of cortisol abundance over 1.5 d (Fig. 1*E*, *Lower*). Although we used cortisol peak time for this purpose, we did not detect a significant difference when we determined the expected body time based on dim-light melatonin onset (DLMO) (*SI Results and Discussion*). Each sample showed a wide range of expected body time. For example, some samples showed expected body time that is almost identical to the sampled time (Fig. 3*A*, black bars), whereas one showed expected body time that was almost antiphasic to the sampled time (Fig. 3*A*, white bar). Remaining samples showed expected body time with an intermediate difference from the sampled time (Fig. 3*A*, gray bars). The observed variability did not result from errors of the conventional method, but reflect individual differences of internal body time because each sample showed similar expected body time when calculated from the 1.5-d time-course abundance data of melatonin (Fig. S2*A*). Accordingly, we categorized nine sample sets into three groups on the basis of the magnitude of the differences between expected body time based on a cortisol rhythm and sampled times: small shift group (CR1 of subject F; CR2 of subjects B and C), moderate shift group (CR1 of subjects D and E; CR2 of subjects A, D, and F), and large shift group (CR2 of subject E).

Next, we calculated the "estimated body time" for each sample set (Fig. 3 *B*–*E* and Table S1 and Figs. S2 *B* and *C*) by our molecular timetable method using the constructed reference metabolite timetable of human blood (Fig. 2). For body-time estimation, we used only two samples of blood drawn 12 h apart. We derived 11 estimated body-time values for each sample set consisting of 17 samples (Fig. 3*E*) and then compared the estimated body time with the predetermined expected body time (via conventional method) to evaluate the accuracy of our molecular timetable method. In the small shift group, the differences between estimated and expected body time were within 2 h (Fig. 3 *B* and *E*). The result was comparable to the previous study using mouse blood samples (12). In the moderate shift group, the differences were within 3 h (Fig. 3 *C* and *E*) and in the large shift group, the differences were about 3 h (Fig. 3 *D* and *E*). In these two groups, the differences were larger than the small shift group. However, in the moderate shift groups, only 3 time points (out of 55) differed by more than 2 h. The time difference of this method (<3 h) is less than the range of the internal body time of shift workers (27, 28). These results suggest that our molecular timetable method can correctly detect shifts of internal body time.

Identification of Metabolites with Circadian Oscillation. Identification of the circadian-oscillating metabolites is important for connecting our current metabolite timetable of human blood to previously reported circadian biology in humans. Identification is also important for further development of our method because once a metabolite is identified, we can update the circadian-metabolite reference list in our human blood timetable, which will improve the sensitivity and specificity of the molecular timetable (12, 42). Therefore, we attempted to identify several circadian-oscillating metabolites in constructing our metabolite timetable and found that a large fraction belong to the steroid hormone metabolism pathway (Fig. 4 and Fig. S3 *A* and *B*). These include cortisol (Fig. 4*A*), cortisone (Fig. 4*B*), urocortisone-3-glucuronide (Fig. 4*C*), pregnanolone sulfate-like metabolite (Fig. 4*D*), and urocoritsol-3-glucuronide (Fig. 4*E*) as well as the amino acids, phenylalanine (Fig. 4*F*), tryptophan (Fig. 4*G*), and leucine (Fig. 4*H*). Cortisol is a well-known circadian-oscillating metabolite in the blood (11), and cortisone is a direct metabolite of the cortisol also found in the blood (49). Urocortisone-3-glucuronide and urocortisol-3-glucuronide are glucuronide forms of urocortisone and urocortisol, respectively, which are downstream metabolites of cortisol and cortisone. A pregnanolone isomer and its precursor (progesterone) were also found as circadian-oscillating metabolites in the brain and blood (50). The circadian oscillations in the human blood of cortisol and cortisone were also detected in the recent report about the human circadian metabolome (13). The peak times (PT) of the cortisol, cortisone, and urocortisone-3-glucuronide were around the afternoon (PT12–PT15; we defined PT12 as noon), and peak times were aligned catabolically according to the steroid metabolism pathway from upstream to downstream (Fig. S3*E*). The peak time of the corticosterone in the mouse plasma samples was CT11.7 (corresponding to PT17.7 in this human study, because both CT6 and PT12 indicate noon) in our previous study (12), and is ~3–6 h later than human peak time. The amino acids, phenylalanine, tryptophan, and leucine were also identified as oscillating metabolites in our mouse plasma study (12), and peak times in mouse and human plasma were ZT18.7–18.9 (corresponding to

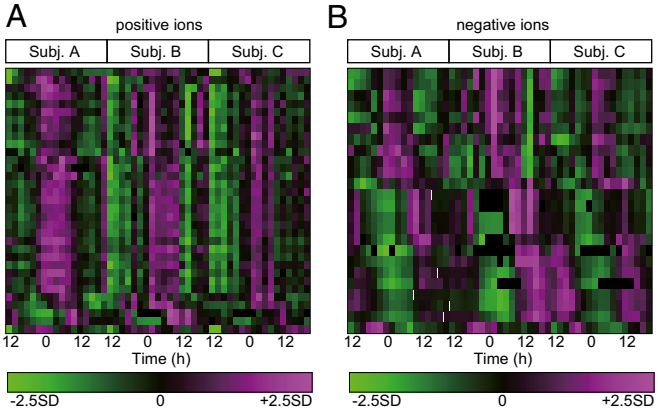

Fig. 2. Heat maps of circadian-oscillating metabolites in the human timetable. Circadian-oscillating metabolite peaks in the plasma samples [positive ions (*A*); negative ions (*B*)] are shown. Some metabolites in this heat map were identified and shown in Fig. 4. On the heat maps, magenta tiles indicate a high quantity of substances and green tiles indicate a low quantity in plasma. Metabolites are sorted according to their molecular peak time.

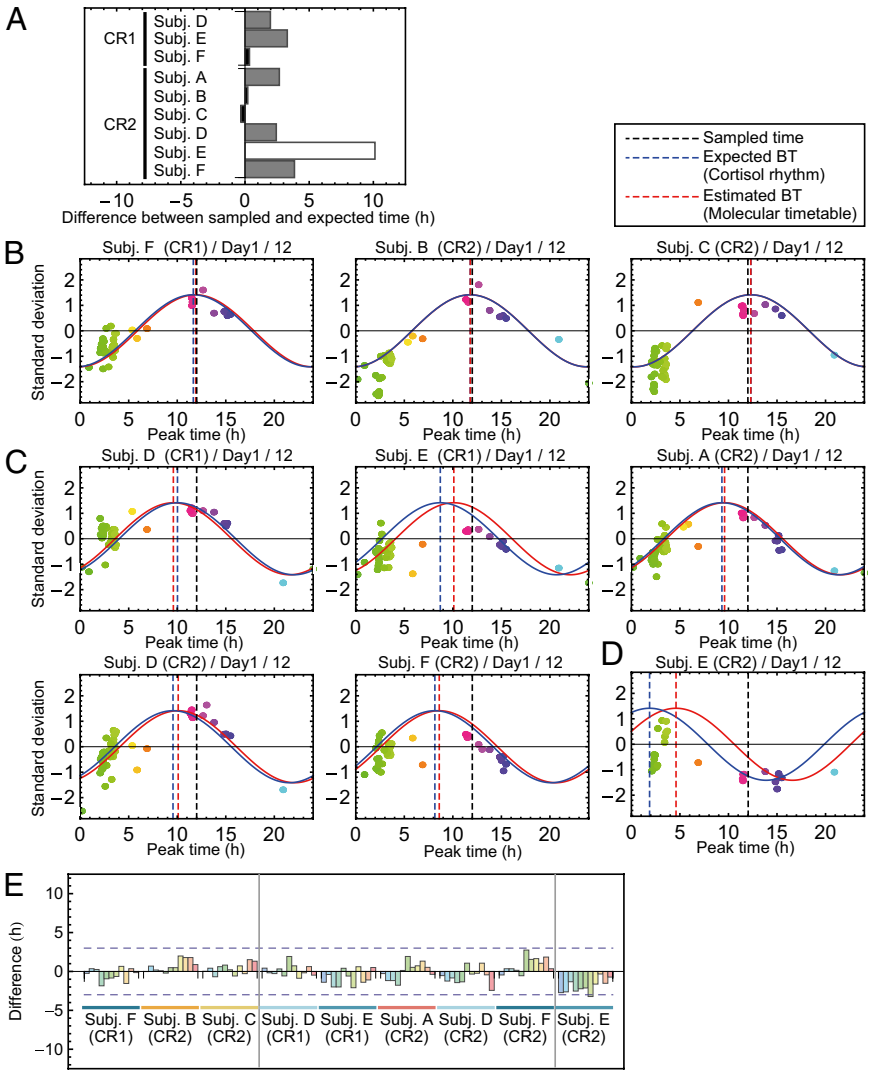

Fig. 3. Estimation of human body time. (*A*) Difference between expected body time and sampled time. Nine sample sets for body-time estimation were classified into three groups by the magnitude of the difference: small (black), moderate (gray), and large (white). (*B–D*) Body-time estimation at 12 h on the first day for nine sample sets in small (*B*), moderate (*C*), and large (*D*) body-time difference groups. Colors of the dots indicate the molecular peak times of each metabolite. Peak time of the red cosine curves indicates estimated body time and peak time of the blue indicates the time of the expected body time. The smaller the distance between red and blue curves, the greater the accuracy of the measurement. Dashed vertical lines show the estimated body time (red), expected body time (blue), or the time the sample was taken (black). In all subjects, expected body time (based on cortisol rhythm) and estimated body time (based on molecular timetable) were similar, indicated by the close proximity of the blue and red dashed lines. (*E*) Summary of body-time estimation. Difference between expected and estimated body time for all estimated samples is shown. The leftmost three samples were ones in the small difference group, the middle five samples were in the moderate difference group, and the rightmost sample was in the large difference group. All samples estimated internal body time within or around 3-h differences between expected and estimated body time. BT, body time.

PT0.7–0.9 in this human study because both ZT6 and PT12 indicate noon), and PT2.2–3.1, respectively, which might reflect the similarity in the phase of the central clock between diurnal and nocturnal animals (51–56).

We also found several lipids among oscillating metabolites, although these metabolites had weak amplitude and/or high variability among individuals (Fig. S3 *A–D*). These lipids include PG(18:1(9Z)/0:0), a glycerophospholipid (Fig. S3*C*), and LysoPC (16:0), a lysophospholipid (Fig. S3*D*). Peak times of these metabolites differed: PT12.0 [PG(18:1(9Z)/0:0)], and PT3.2 [LysoPC (16:0)]. Lysophospholipids also showed circadian oscillation in mouse plasma (12), but their peak time was almost antiphasic (ZT8 in mice corresponding to PT14 in this study), which might reflect the differences between human diurnality and murine nocturnality.

The comparison of our identified circadian-oscillating metabolites to recent studies (13, 14) is explained in *SI Results and Discussion*.

Discussion

In this study, we constructed a human blood metabolite timetable from three individuals, and applied it to these individuals and three other individuals after a forced desynchronization protocol. We successfully detected internal body time in all individuals, even in the different experimental conditions (Fig. S4), which suggests the robustness of our metabolite-timetable method against individual genetic differences. Interestingly, some individuals such as subjects E and F showed 6.8-h and 3.5-h delayed internal body time in constant routine 2 after they experienced a semiconstant routine of enforced 28-h sleep–wake cycles, in comparison with those in constant routine 1 (Fig. 3*A*). Importantly, these delays after enforced sleep–wake cycles were successfully detected by using our metabolite timetable method (Fig. 3 *C* and *D*). These results suggest that the molecular timetable method has potential to be a body-time estimation tool for humans in both normal and abnormal environments like enforced sleep–wake cycles.

Abnormal environments such as shift working, jet lag, and other irregular lifestyles, cause changes in the internal body time of individuals (57). In addition to abnormal environments, genetic differences such as familial advanced sleep phase syndrome (FASPS) also cause changes in the internal body time of individuals (58–60). Brown et al. recently developed a method to potentially detect the circadian rhythm disorders caused by genetic differences (61, 62). They collected skin samples from human subjects, cultured these cells, and transfected them with a clock-controlled reporter to characterize the features of the molecular clock in these tissues. They found that the circadian rhythmicity in isolated cells is correlated with the chronotypes of the subjects, implying that the method could detect circadian rhythm disorders caused by genetic differences. Our molecular

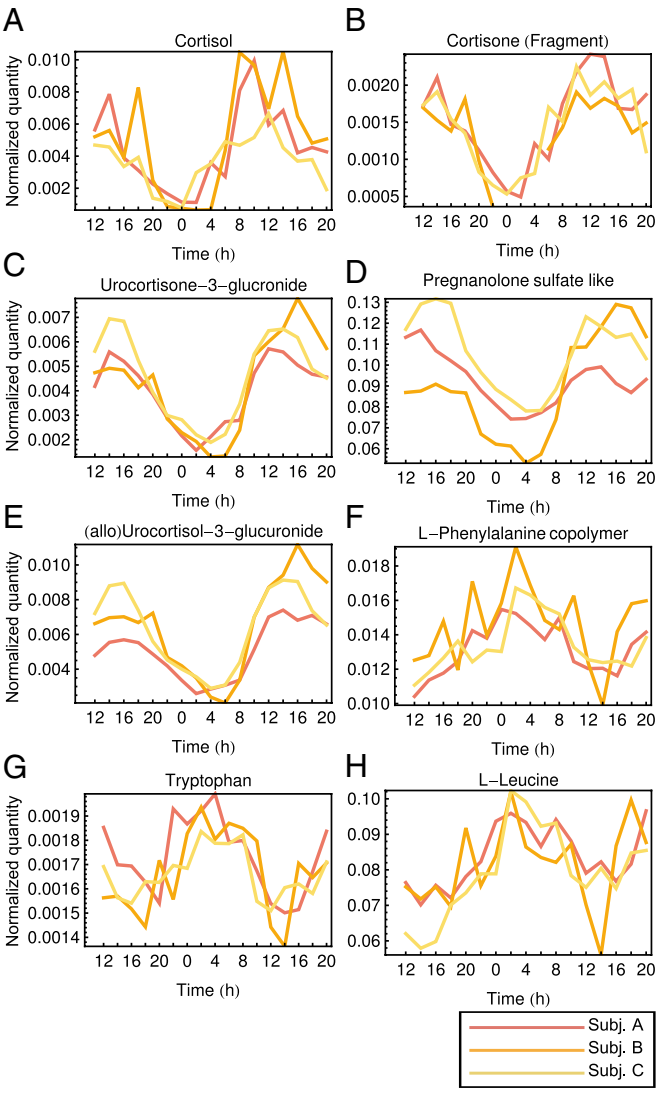

Fig. 4. Identified circadian-oscillating metabolites. Abundance is shown of cortisol (*A*), cortisone (*B*), urocortisone-3-glucuronide (*C*), pregnanolone sulfate-like metabolite (*D*), (allo)urocortisol-3-glucuronide (*E*), L-phenylalanine (*F*), tryptophan (*G*), and L-leucine (*H*) in the blood sampled from three subjects (subject A, subject B, and subject C) whose CR1 samples were used in the metabolite timetable construction. *X* axes show the sampled time from 12 h on day 2 to 20 h on day 3 in CR1, and *y* axes show area of the corresponding peak in the LC–MS analysis.

timetable method can detect both genetic and environmental circadian rhythm disorders, but cannot distinguish between them, whereas Brown et al.'s method can detect genetic but not acquired disorders. These two methods are therefore complementary for detecting circadian rhythm disorders. Our metabolite timetable method may provide a good platform for the initial screening of body-time abnormality caused by either abnormal environments or genetic differences, because our method is minimally invasive and less labor intensive compared with the conventional method or biopsy adopted in Brown et al. (61, 62). Moreover, the metabolite timetable method can track the transient dynamics of internal body time, which cannot be detected by conventional time-course sampling method. It will be interesting in the future to determine whether our timetable method can detect internal body time differences caused by such abnormal environments or genetic differences.

In this study, we used metabolites in blood to detect the internal body time. We note that a molecular timetable concept can be applied not only for circadian-oscillating metabolites, but also for other circadian-oscillating substances (12, 42) and in other tissues like human hair follicle cells from the head or chin (63). Comparing molecular timetable methods with different reference molecules such as clock-controlled RNAs in humans will be of interest to reveal internal synchronization (or desynchronization) between different peripheral clocks such as blood clocks and skin clocks.

In summary, our study shows the possibility that a metabolic molecular timetable can be a convenient diagnostic tool. A minimally invasive internal body-time detection method is essential for facilitating the development of chronotherapy to realize tailored medication regimens as well as for efficient time-restricted feeding to avoid or cure obesity. To measure the abundance of metabolites for body-time estimation, we used LC–MS analysis, which is rarely implemented in current clinical hospitals. However, bench-top MS machines are beginning to appear, and they might be available at hospitals in the future as a routine diagnostic tool; additionally, it may be possible to develop a simpler diagnosis kit using antibodies against a subset of selected circadian metabolites. In any case, our method is more pragmatic than serial time-course sampling because only a few samples are required for body-time estimation and because blood is an easy tissue to sample and analyze. Moreover, our timetable is robust against personal differences because we selected metabolites that oscillated independently of the individual, food intake, sleep, light, and temperature. Thus, the metabolite timetable proposed in this study will provide a convenient way to estimate human body time and may lead to highly optimized and personalized medicine in the future.

Materials and Methods

Subjects. Six healthy, male volunteers, aged 20–23 y (mean age 21.5 y) participated in this study. Subjects had regular sleep–wake patterns, normal hematology, and urinalysis data, and no history of psychiatric disease (assessed by the Mini-International Neuropsychiatric Interview) or severe physical disease. Written informed consent was obtained from each subject. See *SI Materials and Methods* for details.

Measurement of Metabolites. The LC system used was an Agilent 1290 infinity HPLC (Agilent Technologies) with the KEIO MasterHands software (64). See *SI Materials and Methods* for details about the sample preparation, measurements, and data preprocessing.

Construction of Molecular Timetable. We chose peaks that were detected and associated at nine or more time points in all three subjects (subjects A–C) in CR1. For each chosen peak, we performed two statistical tests for selecting candidates for the timetable. See *SI Materials and Methods* for details.

Body-Time Estimation. Body-time estimation was performed as described for the previous mouse blood study (12). Expected body time of nine sample sets for body-time estimation (subjects D–F during CR1, and all six subjects during CR2) were determined on the basis of peak times of the cortisol rhythms (Fig. 1*D*, *Lower*). See *SI Materials and Methods* for details.

MS Identification of Oscillating Metabolites. LC MS/MS analysis was performed for unknown peak identification based on the method described previously (12) with slight modification. See *SI Materials and Methods* for details.

Ethics. The study was approved by RIKEN Kobe Institute Research Ethics Committee (KOBE-IRB-09-07) and the ethics committee of the National Center of Neurology and Psychiatry (22–1-4). All participants have given written consent for the use of material for this research purpose.

ACKNOWLEDGMENTS. We thank Shinobu Abe and Yasuko Sakaguchi at the Institute for Advanced Biosciences (IAB) for metabolomic analysis; Masahiro Hayashi, Hiroshi Fujishima, and Tomoyo Hashiguchi at RIKEN Center for Developmental Biology (CDB) for handling samples; Hiroyuki Tamiya and Ryohei Narumi at RIKEN CDB for helpful discussion; Arthur Millius at RIKEN

CDB for helpful discussion and for proofreading of the manuscript; and Takuro Ito at IAB, Keio University for providing materials used in the identification of oscillating metabolites. This research was supported by an intramural grant-in-aid from the RIKEN CDB (to H.R.U.), research funds from New Energy Developing Organization (to H.R.U.), research funds from the Yamagata Prefectural Government and the city of Tsuruoka (to M.S., M.M., and T.S.), a grant-in-aid for the Strategic Research Program for Brain Sciences from the Ministry of Education, Culture, Sports, Science and Technology of Japan (to K.M.), an Intramural Research Grant (No. 23-3) for Neurological and Psychiatric Disorders of National Center of Neurology and Psychiatry, and a Grant-in Aid for Scientific Research (No. 21390335) from Japan Society for the Promotion of Science (to K.M. and A.H.).

1. Dunlap JC, Loros JJ, DeCoursey PJ, eds (2004) *Chronobiology: Biological Timekeeping* (Sinauer, Sunderland, MA).
2. Hastings MH, Maywood ES, O'Neill JS (2008) Cellular circadian pacemaking and the role of cytosolic rhythms. *Curr Biol* 18:R805–R815.
3. Akhtar RA, et al. (2002) Circadian cycling of the mouse liver transcriptome, as revealed by cDNA microarray, is driven by the suprachiasmatic nucleus. *Curr Biol* 12:540–550.
4. Panda S, et al. (2002) Coordinated transcription of key pathways in the mouse by the circadian clock. *Cell* 109:307–320.
5. Storch KF, et al. (2002) Extensive and divergent circadian gene expression in liver and heart. *Nature* 417:78–83.
6. Ueda HR, et al. (2002) A transcription factor response element for gene expression during circadian night. *Nature* 418:534–539.
7. Reppert SM, Weaver DR (2002) Coordination of circadian timing in mammals. *Nature* 418:935–941.
8. Ueda HR (2007) Systems biology of mammalian circadian clocks. *Cold Spring Harb Symp Quant Biol* 72:365–380.
9. Takahashi JS, Hong HK, Ko CH, McDearmon EL (2008) The genetics of mammalian circadian order and disorder: Implications for physiology and disease. *Nat Rev Genet* 9:764–775.
10. Kennaway DJ, Voultsios A, Varcoe TJ, Moyer RW (2002) Melatonin in mice: Rhythms, response to light, adrenergic stimulation, and metabolism. *Am J Physiol Regul Integr Comp Physiol* 282:R358–R365.
11. Weitzman ED, et al. (1971) Twenty-four hour pattern of the episodic secretion of cortisol in normal subjects. *J Clin Endocrinol Metab* 33:14–22.
12. Minami Y, et al. (2009) Measurement of internal body time by blood metabolomics. *Proc Natl Acad Sci USA* 106:9890–9895.
13. Dallmann R, Viola AU, Tarokh L, Cajochen C, Brown SA (2012) The human circadian metabolome. *Proc Natl Acad Sci USA* 109:2625–2629.
14. Eckel-Mahan KL, et al. (2012) Coordination of the transcriptome and metabolome by the circadian clock. *Proc Natl Acad Sci USA* 109:5541–5546.
15. Fustin JM, et al. (2012) Rhythmic nucleotide synthesis in the liver: temporal segregation of metabolites. *Cell Rep* 1:341–349.
16. Halberg F (1969) Chronobiology. *Annu Rev Physiol* 31:675–725.
17. Labrecque G, Bélanger PM (1991) Biological rhythms in the absorption, distribution, metabolism and excretion of drugs. *Pharmacol Ther* 52:95–107.
18. Lemmer B, Scheidel B, Behne S (1991) Chronopharmacokinetics and chronopharmacodynamics of cardiovascular active drugs. Propranolol, organic nitrates, nifedipine. *Ann N Y Acad Sci* 618:166–181.
19. Reinberg A, Halberg F (1971) Circadian chronopharmacology. *Annu Rev Pharmacol* 11:455–492.
20. Reinberg A, Smolensky M, Levi F (1983) Aspects of clinical chronopharmacology. *Cephalalgia* 3(Suppl 1):69–78.
21. Bocci V (1985) Administration of interferon at night may increase its therapeutic index. *Cancer Drug Deliv* 2:313–318.
22. Ohdo S, Koyanagi S, Suyama H, Higuchi S, Aramaki H (2001) Changing the dosing schedule minimizes the disruptive effects of interferon on clock function. *Nat Med* 7: 356–360.
23. Lévi F, Zidani R, Misset JL; International Organization for Cancer Chronotherapy (1997) Randomised multicentre trial of chronotherapy with oxaliplatin, fluorouracil, and folinic acid in metastatic colorectal cancer. *Lancet* 350:681–686.
24. Hrushesky WJ (1985) Circadian timing of cancer chemotherapy. *Science* 228:73–75.
25. Wright KP, Jr., Gronfier C, Duffy JF, Czeisler CA (2005) Intrinsic period and light intensity determine the phase relationship between melatonin and sleep in humans. *J Biol Rhythms* 20:168–177.
26. Hasan S, et al. (2012) Assessment of circadian rhythms in humans: Comparison of real-time fibroblast reporter imaging with plasma melatonin. *FASEB J* 26:2414–2423.
27. Horowitz TS, Cade BE, Wolfe JM, Czeisler CA (2001) Efficacy of bright light and sleep/darkness scheduling in alleviating circadian maladaptation to night work. *Am J Physiol Endocrinol Metab* 281:E384–E391.
28. Smith MR, Eastman CI (2008) Night shift performance is improved by a compromise circadian phase position: Study 3. Circadian phase after 7 night shifts with an intervening weekend off. *Sleep* 31:1639–1645.
29. Arble DM, Bass J, Laposky AD, Vitaterna MH, Turek FW (2009) Circadian timing of food intake contributes to weight gain. *Obesity (Silver Spring)* 17:2100–2102.
30. Hatori M, et al. (2012) Time-restricted feeding without reducing caloric intake prevents metabolic diseases in mice fed a high-fat diet. *Cell Metab* 15:848–860.
31. Rutter J, Reick M, McKnight SL (2002) Metabolism and the control of circadian rhythms. *Annu Rev Biochem* 71:307–331.
32. Yang X, et al. (2006) Nuclear receptor expression links the circadian clock to metabolism. *Cell* 126:801–810.
33. Froy O (2007) The relationship between nutrition and circadian rhythms in mammals. *Front Neuroendocrinol* 28:61–71.
34. Green CB, Takahashi JS, Bass J (2008) The meter of metabolism. *Cell* 134:728–742.
35. Alenghat T, et al. (2008) Nuclear receptor corepressor and histone deacetylase 3 govern circadian metabolic physiology. *Nature* 456:997–1000.
36. Nakahata Y, et al. (2008) The NAD+-dependent deacetylase SIRT1 modulates CLOCK-mediated chromatin remodeling and circadian control. *Cell* 134:329–340.
37. Le Martelot G, et al. (2009) REV-ERBalpha participates in circadian SREBP signaling and bile acid homeostasis. *PLoS Biol* 7:e1000181.
38. Vollmers C, et al. (2009) Time of feeding and the intrinsic circadian clock drive rhythms in hepatic gene expression. *Proc Natl Acad Sci USA* 106:21453–21458.
39. Zhang EE, et al. (2010) Cryptochrome mediates circadian regulation of cAMP signaling and hepatic gluconeogenesis. *Nat Med* 16:1152–1156.
40. Froy O (2010) Metabolism and circadian rhythms—implications for obesity. *Endocr Rev* 31:1–24.
41. Bass J, Takahashi JS (2010) Circadian integration of metabolism and energetics. *Science* 330:1349–1354.
42. Ueda HR, et al. (2004) Molecular-timetable methods for detection of body time and rhythm disorders from single-time-point genome-wide expression profiles. *Proc Natl Acad Sci USA* 101:11227–11232.
43. Masumoto KH, et al. (2010) Acute induction of Eya3 by late-night light stimulation triggers TSHβ expression in photoperiodism. *Curr Biol* 20:2199–2206.
44. Plumb R, et al. (2003) Metabonomic analysis of mouse urine by liquid-chromatography-time of flight mass spectrometry (LC-TOFMS): Detection of strain, diurnal and gender differences. *Analyst (Lond)* 128:819–823.
45. Wilson ID, et al. (2005) High resolution "ultra performance" liquid chromatography coupled to oa-TOF mass spectrometry as a tool for differential metabolic pathway profiling in functional genomic studies. *J Proteome Res* 4:591–598.
46. Tolstikov VV, Lommen A, Nakanishi K, Tanaka N, Fiehn O (2003) Monolithic silica-based capillary reversed-phase liquid chromatography/electrospray mass spectrometry for plant metabolomics. *Anal Chem* 75:6737–6740.
47. Mills JN, Minors DS, Waterhouse JM (1978) Adaptation to abrupt time shifts of the oscillator(s) controlling human circadian rhythms. *J Physiol* 285:455–470.
48. Czeisler CA, et al. (1999) Stability, precision, and near-24-hour period of the human circadian pacemaker. *Science* 284:2177–2181.
49. Nuller YL, Morozova MG, Kushnir ON, Hamper N (2001) Effect of naloxone therapy on depersonalization: A pilot study. *J Psychopharmacol* 15:93–95.
50. Corpéchot C, et al. (1997) Brain neurosteroids during the mouse oestrous cycle. *Brain Res* 766:276–280.
51. Inouye ST, Kawamura H (1979) Persistence of circadian rhythmicity in a mammalian hypothalamic "island" containing the suprachiasmatic nucleus. *Proc Natl Acad Sci USA* 76:5962–5966.
52. Kubota A, Inouye ST, Kawamura H (1981) Reversal of multiunit activity within and outside the suprachiasmatic nucleus in the rat. *Neurosci Lett* 27:303–308.
53. Nunez AA, Bult A, McElhinny TL, Smale L (1999) Daily rhythms of Fos expression in hypothalamic targets of the suprachiasmatic nucleus in diurnal and nocturnal rodents. *J Biol Rhythms* 14:300–306.
54. Schwartz MD, Nunez AA, Smale L (2004) Differences in the suprachiasmatic nucleus and lower subparaventricular zone of diurnal and nocturnal rodents. *Neuroscience* 127:13–23.
55. Ramanathan C, Nunez AA, Martinez GS, Schwartz MD, Smale L (2006) Temporal and spatial distribution of immunoreactive PER1 and PER2 proteins in the suprachiasmatic nucleus and peri-suprachiasmatic region of the diurnal grass rat (Arvicanthis niloticus). *Brain Res* 1073–1074:348–358.
56. Ramanathan C, Stowie A, Smale L, Nunez AA (2010) Phase preference for the display of activity is associated with the phase of extra-suprachiasmatic nucleus oscillators within and between species. *Neuroscience* 170:758–772.
57. Duffy JF, Czeisler CA (2009) Effect of light on human circadian physiology. *Sleep Med Clin* 4:165–177.
58. Jones CR, et al. (1999) Familial advanced sleep-phase syndrome: A short-period circadian rhythm variant in humans. *Nat Med* 5:1062–1065.
59. Toh KL, et al. (2001) An hPer2 phosphorylation site mutation in familial advanced sleep phase syndrome. *Science* 291:1040–1043.
60. Xu Y, et al. (2005) Functional consequences of a CKIdelta mutation causing familial advanced sleep phase syndrome. *Nature* 434:640–644.
61. Brown SA, et al. (2005) The period length of fibroblast circadian gene expression varies widely among human individuals. *PLoS Biol* 3:e338.
62. Brown SA, et al. (2008) Molecular insights into human daily behavior. *Proc Natl Acad Sci USA* 105:1602–1607.
63. Akashi M, et al. (2010) Noninvasive method for assessing the human circadian clock using hair follicle cells. *Proc Natl Acad Sci USA* 107:15643–15648.
64. Sugimoto M, Wong DT, Hirayama A, Soga T, Tomita M (2010) Capillary electrophoresis mass spectrometry-based saliva metabolomics identified oral, breast and pancreatic cancer-specific profiles. *Metabolomics* 6:78–95.

Supporting Information

Kasukawa et al. 10.1073/pnas.1207768109

SI Results and Discussion

Evaluation of Body-Time Estimation with Dim-Light Melatonin Onset (DLMO). We used cortisol peak times (CPT) for determining the expected body time. However, as DLMO is frequently used to determine human internal body times, we also evaluated our body-time estimation with the expected body time based on DLMO. We first determined DLMO for each constant routine and each subject. The threshold to determine the DLMO for each melatonin profile was set to the average of the five lowest raw data points plus 25% of the average of the five highest raw data points. DLMO was calculated by a linear interpolation between data points just above and below this threshold. Next the expected body times were determined on the basis of the DLMO with the same method for CPT (Fig. S4*A*). With this expected body time based on DLMO, we reevaluated our body-time estimation (Fig. S4*B*). Although there were some additional data points at which the time differences were more than 3 h (one time point in CPT and three time points in DLMO), the time differences based on DLMO were not significantly different from CPT because the *P* value of the Wilcox rank sum test between time differences based on CPT and DLMO was 0.125 (>0.05).

Evaluation of Body-Time Estimation with Single Time Point and Three Time Points. We used blood samples at two antiphasic time points for the body-time estimation in this study. We also evaluated other conditions of the body-time estimation with a sample at one time point and samples at three time points separated by 8 h (one at the target time point, one 8 h later, and one 16 h later). We estimated the body times from 1200 hours to 2200 hours on day 1 and from 0000 hours to 0600 hours on day 2 in CR1 (subjects D–F) and CR2 (subjects A–F) for every condition. The result is summarized in Fig. S4*C*. With one time-point sampling, the time differences were larger than in two time-point sampling. With three time-point sampling, the time differences were similar to two time-point sampling. This result suggests that one time-point sampling is difficult to use for body-time estimation with the current method and technology, but that both two and three time-point samplings are practical. The accuracy in the one time-point method could be improved if the quantitativeness and reproducibility of the MS measurements is improved in the future.

Bias in Selection of Subjects for the Molecular Timetable Construction. In our timetable construction, we chose subjects (A–C) whose body time most closely matched each other and previously reported melatonin and cortisol rhythms. However, there is a possibility of inherent bias in selecting the "best" three subjects. Consequently, we constructed molecular timetables from all combinations of three subjects (A–F) and performed body-time estimation of the other samples (that is, 99 time points in total) that were not used in molecular timetable construction. Fig. S4*D* shows the result of this evaluation. Although there were some outlier estimations, 75% of all body-time estimations showed less than 2-h differences in almost all combinations of subjects, and no strong bias in choosing subjects A, B, and C for the timetable construction seems to be detected. In the combinations of subjects (A, D, and E), (B, D, and E), and (C, D, and E), the estimation results were a bit worse than the other combinations. This may reflect the fact that subjects D and E in CR1 had more shifts than the other four subjects. These results suggest that the selection of the subjects for the molecular timetable construction in this study is appropriate.

Effect of Food Intake in Body-Time Estimation. Although we did not directly evaluate the effect of food intake, we minimized the effect of food intake as much as possible. In the molecular timetable construction, we used blood samples drawn from subjects under constant routine, in which foods were taken every 2 h during sampling periods, and blood samples were collected just before food intake every time to keep diet effects as low as possible. This allowed us to exclude metabolites whose circadian oscillations were driven by the dietary cycle. Furthermore, we excluded circadian oscillating metabolite peaks with variability among individuals. This enabled us to remove some metabolites that were affected by food intake. For example, we could detect several lipids among 310 circadian oscillating peaks (142 positive and 168 negative ion peaks) such as SM(d18:1/18:1), PC(18:2/18:2), and LysoPC(16:0), but ultimately all were excluded except one lipid Cer(d18:2/16:0) based on individual variability. The reason for such variation in the lipid profiles may be that the subjects took different foods in the constant routines, which may weaken the effects of specific foods and ingredients. Thus, we believe that the effect of food intake in our body-time estimation was minimized to some extent.

Comparison of Identified Circadian-Oscillating Metabolites in This Study to Other Studies. Two recent studies identified circadian-oscillating metabolites in humans (1) and in mice (2). In the Dallmann et al. study (1), they identified 41 metabolites in human plasma and 29 metabolites in human saliva. There are a few common plasma circadian metabolites that were identified both in their study and ours, for example, cortisol and cortisone. Meanwhile, 33 of 41 plasma circadian metabolites were lipids in their study but only one metabolite in our timetable was a lipid. The difference may be caused by our timetable construction method to exclude metabolite peaks exhibiting variability among individuals. We did find several lipids, but they were excluded on the basis of variation between individuals (Dataset S1). In Eckel-Mahan's study (2), they identified 60 circadian metabolites in mouse liver. Although some circadian-oscillating amino acids were identified in both their study and ours, there were no common metabolites. This may be because the targeted organs were different (plasma and liver), different conditions were used in the mass-spectrometry analysis, or because many of our circadian-oscillating metabolites remain unidentified.

In this study, the number of metabolite peaks (58 peaks) with circadian fluctuations was smaller and the false discovery rate (FDR) cutoff (0.1) was higher than our previous mouse study (3). This is because our changed method for choosing circadian metabolite peaks in the human molecular timetable is different. In the mouse study, we fitted cosine curves to abundances of time-course metabolite peak areas and chose ones with FDR $\leq$0.01 using shape information only. This was possible because the duration of our mouse study was 96 h (light-dark condition 48 h and dark-dark condition 48 h) compared with 34 h in this study. This probably decreases the sensitivity of selecting circadian metabolites. To overcome this issue, we chose metabolite peaks for the human metabolite molecular timetable using two criteria—shapes and amplitude—with relaxed cutoff scores (FDR $\leq$ 0.1). Although each cutoff is higher (0.1) than the one used in the mouse study, the overall cutoff is $0.1 \times 0.1 = 0.01$ because metabolite peaks were filtered by two independent criteria (FDR $\leq$ 0.1), which is equivalent to FDR $\leq$ 0.01 used in the mouse study.

SI Materials and Methods

Sampling. All subjects participated in a 13-d forced desynchronization (FD) protocol in a temporal isolation laboratory free from external time cues. Subjects entered individual rooms in the sleep laboratory (5.9 m^2 polysomnographic bedroom, 67.9 m^2 living room, restroom, and bathroom) at 1700 hours on day 1. After having a meal and taking a bath, they turned the lights off and went to bed at 2400 hours and slept for 9 h 20 min on a bed in an individual room. The FD protocol used in this study was conducted entirely in the laboratory and was composed of the following three studies: (*i*) measurement under a constant routine condition (CR1) (4) followed by (*ii*) a 28-h sleep–wake schedule for 7 d (5), and (*iii*) a second measurement under CR2. The 28-h sleep–wake schedule included 9 h 20 min of sleep (promoting sleep/bedrest with lights off) and 18 h 40 min of wakefulness (prohibiting sleep). During the FD protocol, subjects stayed in the laboratory in isolation from external time cues such as clock, radio, newspaper, cell phone, and Internet access. They were asked to maintain wakefulness under a low-intensity light condition (<15 lx) during the scheduled wake period and to sleep in the bedroom with the lights off (0 lx) during the sleep period. Throughout the study, subjects were under constant surveillance by seven researchers and were verbally awakened when they unintentionally took a nap during the wake period. During the wake period, however, they were allowed to move freely around in the laboratory, read and write, enjoy music and videos, play videogames, and engage in conversation with a researcher. Ambient temperature and humidity in the laboratory were maintained at 25 ± 0.5 °C and 50 ± 5% relative humidity (RH), respectively. During the constant routine conditions, subjects were required to lie on a reclining chair in a supine position and stay awake for 38 h 40 min. Blood was collected every 2 h using an i.v. catheter placed in a forearm vein of the subject. Water was available at all times and a 200-kcal meal was provided every 2 h. The protocol was approved by the institutional ethics committee of the National Center of Neurology and Psychiatry and was conducted in accordance with the Declaration of Helsinki.

Measuring Cortisol and Melatonin in the Blood. Plasma was isolated from whole blood by centrifugation. Plasma melatonin and cortisol levels at each time point were measured using RIA (Bühlmann Lab).

LC–MS Measurement. To 30 μL of the plasma samples, 270 μL of isopropyl alcohol containing an internal standard (2.2 μmol/L of camphor-10-sulfonic acid) was added with shaking. The mixture was centrifuged at 20,400 × *g* for 10 min at 4 °C, and the supernatant was then transferred to another tube and vacuum dried at 35 °C. The samples were mixed with Milli-Q water and chloroform in a volume ratio of 2:4:1 containing 20 μmol/L of 3,5-di-tert-butyl-4-hydroxyhydrocinnamate, centrifuged at 20,400 × *g*, for 5 min at 4 °C, and 25 μL of the supernatant was used for LC–TOF/MS analysis.

The LC system was an Agilent 1290 infinity HPLC (Agilent Technologies). The Acquity ultra performance liquid chromatography BEH C18 (1.7 μm, 2.1 mm × 50 mm) column was purchased from Waters, and was maintained at 50 °C. The mobile phase consisted of 0.5% acetic acid/water as eluent A and isopropanol as eluent B. The gradient was linearly changed from solvent (A/B = 99/1, vol/vol) to solvent (A/B = 1/99, vol/vol) for 12 min and held for 5 min. The flow rate was 0.3 mL/min and the injection volume was 1 μL. MS data were acquired on a 6530 Accurate-Mass Q-TOF LC/MS using the dual spray ESI of G-3251A (Agilent). Samples were analyzed by both positive and negative ion electrospray mass spectrometry. The MS conditions used were as follows: gas temperature 350 °C, drying gas 10 L/min, nebulizer 30 psig, fragmentor 200 V, skimmer 90 V, OCT1 RF Vpp 250 V, scan range *m/z* 100–1,600 and nozzle voltage 1,000 V. The capillary voltages were 3.5 and 4.0 kV for negative and positive mode, respectively.

Peak Association. We used two peak association algorithms for intraseries peaks and for interseries peaks. The algorithm for intraseries peaks was used for associating peaks obtained from 17 samples taken from each subject in any of two constant routines (CR1 or CR2). For the intraseries peak association, we used the KEIO MasterHands software (6), in which both automated algorithm and manual curation can be performed. For the interseries peak association, we first corrected retention time (RT) according to the reported method (7), then we associated the peaks in two series with the smallest values of: (difference of *m/z* between 2 series/X)^2 + (difference of RT between 2 series/Y)^2 in peaks with (difference of *m/z*) < X and (difference of RT) < Y in both series. Parameters X and Y were 0.02 and 0.25, respectively.

Normalization. Each peak area was first normalized by the area of the internal standard (camphor-10-sulfonic acid) spiked into each sample. After this normalization, we also performed a second normalization as follows:

In the second normalization process (normalization of area distribution), we first selected one (centroid) sample from all samples (this centroid sample had the largest mean of Pearson's correlations with the other samples). Centroid samples were independently chosen for positive and negative ion data. Then, for each sample, linear regression to the function $Y = aX + b$ was performed with all log areas of the target (Y) and centroid (X) samples, and areas of the target samples normalized according to the fitted linear function by subtracting the fitted value b and divided by a from the target areas (Y), resulting in the normalized target area ($Y' = (Y - b)/a$).

Construction of Molecular Timetable. We chose peaks that were detected and associated at nine or more time points in all three subjects (subjects A–C) in CR1. For each chosen peak, we performed two statistical tests for selecting candidates for the timetable. First, we searched for the maximum Pearson's correlation of a cosine curve of a 24-h period to determine the phase using a Fourier transformation-based method (8) to mean area values of three subjects by averaging the area values at the same sampled time. We then estimated P values and FDRs by permutation tests as shown in the previous study (3). Next, we tested significant diurnal changes against the individual difference using one-way ANOVA, in which we grouped samples of three subjects with the same sampled time. We then calculated P values and FDRs. Finally, we selected peaks that have FDR ≤0.1 in both tests as indicators in the human timetable. We focused on cosine-wave–like metabolites, because the estimation of peak time of circadian metabolites of cosine-wave form is not affected by the time points in the construction of metabolite timetable.

Expected Body Time. First, the mean cortisol peak time of the three sample sets that were used in the timetable construction (subjects A–C during CR1) was calculated and defined by standard cortisol peak time (PT11.68). Differences of cortisol peak times for the other nine samples to the standard cortisol peak time were calculated and determined as differences between expected body time and sampled time.

MS Identification of Oscillating Metabolites. LC MS/MS analysis was performed for unknown peak identification based on the method described in the previous report (3) with slight modification. The LC system was an Agilent 1290 infinity HPLC (Agilent Technologies) and the mobile phase consisted of 0.5% acetic acid/water as eluent A and isopropanol as eluent B. MS data were acquired on a 6530 Accurate-Mass Q-TOF LC/MS using the

dual spray ESI of G-3251A (Agilent Technologies). The collision energy was set at a range of 20–60 V. For fragmentation products, the mass range was set between *m/z* 50 and *m/z* 1,000. The peaks at *m/z* 539.255, 395.194, 509.2852, and 541.2705 were identified by comparing their fragmented spectrum. First MS (Q1) selected their ions and the second MS (Q2 or collision cell) observed their fragmented spectrums, and these patterns were compared with those of steroid with glucuronic acid or sulfate and phospholipid. The other peaks at *m/z* 421.2268, 329.1783, 397.2109, 367.1630, 554.3534, 351.1363, 203.0856, and 130.0889 were identified by comparing retention time and fragment pattern with authentic specimen for cortisol, cortisone, pregnenolone-3-sulfate, dehydroepiandrosterone sulfate, lysophosphatidylcholine, L-phenylalanine, L-tryptophan, and L-leucine, respectively.

Image of the Steroid Hormone Pathway. The image of the steroid hormone pathway was generated through the use of IPA (Ingenuity Systems).

1. Dallmann R, Viola AU, Tarokh L, Cajochen C, Brown SA (2012) The human circadian metabolome. *Proc Natl Acad Sci USA* 109:2625–2629.
2. Eckel-Mahan KL, et al. (2012) Coordination of the transcriptome and metabolome by the circadian clock. *Proc Natl Acad Sci USA* 109:5541–5546.
3. Minami Y, et al. (2009) Measurement of internal body time by blood metabolomics. *Proc Natl Acad Sci USA* 106:9890–9895.
4. Mills JN, Minors DS, Waterhouse JM (1978) Adaptation to abrupt time shifts of the oscillator(s) controlling human circadian rhythms. *J Physiol* 285:455–470.
5. Czeisler CA, et al. (1999) Stability, precision, and near-24-hour period of the human circadian pacemaker. *Science* 284:2177–2181.
6. Sugimoto M, Wong DT, Hirayama A, Soga T, Tomita M (2010) Capillary electrophoresis mass spectrometry-based saliva metabolomics identified oral, breast and pancreatic cancer-specific profiles. *Metabolomics* 6:78–95.
7. Reijeng JC, Martens JH, Giuliani A, Chiari M (2002) Pherogram normalization in capillary electrophoresis and micellar electrokinetic chromatography analyses in cases of sample matrix-induced migration time shifts. *J Chromatogr B Analyt Technol Biomed Life Sci* 770:45–51.
8. Chatfield C (1996) *The Analysis of Time Series: An Introduction* (Chapman & Hall/CRC, London), 5th Ed, p 304.

Table S1. Summary of human body-time estimation

Target sample	Antiphasic sample	Shift group	Used peaks	Expected phase	Estimated phase	Difference	Correlation
Subject D/CR1/day1-1200 h	Subject D/CR1/day2-0000 h	Moderate	54	10.0238	9.6	0.4238	0.733
Subject D/CR1/day1-1400 h	Subject D/CR1/day2-0200 h	Moderate	54	12.0238	12.2	0.1762	0.8989
Subject D/CR1/day1-1600 h	Subject D/CR1/day2-0400 h	Moderate	53	14.0238	14.3	0.2762	0.8825
Subject D/CR1/day1-1800 h	Subject D/CR1/day2-0600 h	Moderate	51	16.0238	15.7	0.3238	0.909
Subject D/CR1/day1-2000 h	Subject D/CR1/day2-0800 h	Moderate	55	18.0238	18.6	0.5762	0.6699
Subject D/CR1/day1-2200 h	Subject D/CR1/day2-1000 h	Moderate	55	20.0238	18.1	1.9238	0.7431
Subject D/CR1/day2-0000 h	Subject D/CR1/day2-1200 h	Moderate	54	22.0238	21.3	0.7238	0.7531
Subject D/CR1/day2-0200 h	Subject D/CR1/day2-1400 h	Moderate	54	0.0238	0.9	0.8762	0.8578
Subject D/CR1/day2-0400 h	Subject D/CR1/day2-1600 h	Moderate	53	2.0238	2.2	0.1762	0.8211
Subject D/CR1/day2-0600 h	Subject D/CR1/day2-1800 h	Moderate	51	4.0238	3.4	0.6238	0.7808
Subject D/CR1/day2-0800 h	Subject D/CR1/day2-2000 h	Moderate	55	6.0238	6.5	0.4762	0.6753
Subject E/CR1/day1-1200 h	Subject E/CR1/day2-0000 h	Moderate	54	8.7071	10.1	1.3929	0.6693
Subject E/CR1/day1-1400 h	Subject E/CR1/day2-0200 h	Moderate	53	10.7071	11.1	0.3929	0.9089
Subject E/CR1/day1-1600 h	Subject E/CR1/day2-0400 h	Moderate	51	12.7071	14.7	1.9929	0.9148
Subject E/CR1/day1-1800 h	Subject E/CR1/day2-0600 h	Moderate	53	14.7071	16.7	1.9929	0.8366
Subject E/CR1/day1-2000 h	Subject E/CR1/day2-0800 h	Moderate	54	16.7071	16.3	0.4071	0.9137
Subject E/CR1/day1-2200 h	Subject E/CR1/day2-1000 h	Moderate	54	18.7071	19.3	0.5929	0.7496
Subject E/CR1/day2-0000 h	Subject E/CR1/day2-1200 h	Moderate	54	20.7071	22.8	2.0929	0.7268
Subject E/CR1/day2-0200 h	Subject E/CR1/day2-1400 h	Moderate	53	22.7071	22.1	0.6071	0.6479
Subject E/CR1/day2-0400 h	Subject E/CR1/day2-1600 h	Moderate	50	0.7071	2.1	1.3929	0.8349
Subject E/CR1/day2-0600 h	Subject E/CR1/day2-1800 h	Moderate	53	2.7071	3.8	1.0929	0.8684
Subject E/CR1/day2-0800 h	Subject E/CR1/day2-2000 h	Moderate	54	4.7071	4.2	0.5071	0.8645
Subject F/CR1/day1-1200 h	Subject F/CR1/day2-0000 h	Small	51	11.6539	11.9	0.2461	0.9028
Subject F/CR1/day1-1400 h	Subject F/CR1/day2-0200 h	Small	49	13.6539	13.3	0.3539	0.9321
Subject F/CR1/day1-1600 h	Subject F/CR1/day2-0400 h	Small	50	15.6539	15.4	0.2539	0.9455
Subject F/CR1/day1-1800 h	Subject F/CR1/day2-0600 h	Small	47	17.6539	19.5	1.8461	0.6782
Subject F/CR1/day1-2000 h	Subject F/CR1/day2-0800 h	Small	50	19.6539	20.6	0.9461	0.7647
Subject F/CR1/day1-2200 h	Subject F/CR1/day2-1000 h	Small	51	21.6539	22.5	0.8461	0.7025
Subject F/CR1/day2-0000 h	Subject F/CR1/day2-1200 h	Small	51	23.6539	0.3	0.6461	0.8818
Subject F/CR1/day2-0200 h	Subject F/CR1/day2-1400 h	Small	50	1.6539	1	0.6539	0.9214
Subject F/CR1/day2-0400 h	Subject F/CR1/day2-1600 h	Small	48	3.6539	5.2	1.5461	0.8368
Subject F/CR1/day2-0600 h	Subject F/CR1/day2-1800 h	Small	50	5.6539	5.3	0.3539	0.899
Subject F/CR1/day2-0800 h	Subject F/CR1/day2-2000 h	Small	53	7.6539	7.8	0.1461	0.7676
Subject A/CR2/day1-1200 h	Subject A/CR2/day2-0000 h	Moderate	57	9.3265	9.6	0.2735	0.8654
Subject A/CR2/day1-1400 h	Subject A/CR2/day2-0200 h	Moderate	57	11.3265	12.5	1.1735	0.8876
Subject A/CR2/day1-1600 h	Subject A/CR2/day2-0400 h	Moderate	58	13.3265	14.5	1.1735	0.9425
Subject A/CR2/day1-1800 h	Subject A/CR2/day2-0600 h	Moderate	57	15.3265	17.1	1.7735	0.8419
Subject A/CR2/day1-2000 h	Subject A/CR2/day2-0800 h	Moderate	56	17.3265	17.2	0.1265	0.7339
Subject A/CR2/day1-2200 h	Subject A/CR2/day2-1000 h	Moderate	56	19.3265	17.4	1.9265	0.8632
Subject A/CR2/day2-0000 h	Subject A/CR2/day2-1200 h	Moderate	57	21.3265	20.8	0.5265	0.7902
Subject A/CR2/day2-0200 h	Subject A/CR2/day2-1400 h	Moderate	58	23.3265	22.6	0.7265	0.8653
Subject A/CR2/day2-0400 h	Subject A/CR2/day2-1600 h	Moderate	55	1.3265	0	1.3265	0.8591
Subject A/CR2/day2-0600 h	Subject A/CR2/day2-1800 h	Moderate	57	3.3265	2.8	0.5265	0.7926
Subject A/CR2/day2-0800 h	Subject A/CR2/day2-2000 h	Moderate	54	5.3265	5.7	0.3735	0.57
Subject B/CR2/day1-1200 h	Subject B/CR2/day2-0000 h	Small	52	11.7863	11.8	0.0137	0.9166
Subject B/CR2/day1-1400 h	Subject B/CR2/day2-0200 h	Small	54	13.7863	13.1	0.6863	0.9131
Subject B/CR2/day1-1600 h	Subject B/CR2/day2-0400 h	Small	55	15.7863	15.6	0.1863	0.9319
Subject B/CR2/day1-1800 h	Subject B/CR2/day2-0600 h	Small	55	17.7863	17.7	0.0863	0.9199
Subject B/CR2/day1-2000 h	Subject B/CR2/day2-0800 h	Small	55	19.7863	20	0.2137	0.8265
Subject B/CR2/day1-2200 h	Subject B/CR2/day2-1000 h	Small	55	21.7863	21.3	0.4863	0.8616
Subject B/CR2/day2-0000 h	Subject B/CR2/day2-1200 h	Small	53	23.7863	23.3	0.4863	0.8926
Subject B/CR2/day2-0200 h	Subject B/CR2/day2-1400 h	Small	54	1.7863	23.8	1.9863	0.8588
Subject B/CR2/day2-0400 h	Subject B/CR2/day2-1600 h	Small	55	3.7863	2	1.7863	0.8764
Subject B/CR2/day2-0600 h	Subject B/CR2/day2-1800 h	Small	55	5.7863	4	1.7863	0.8975
Subject B/CR2/day2-0800 h	Subject B/CR2/day2-2000 h	Small	56	7.7863	6.9	0.8863	0.7229
Subject C/CR2/day1-1200 h	Subject C/CR2/day2-0000 h	Small	45	12.316	12.3	0.016	0.8965
Subject C/CR2/day1-1400 h	Subject C/CR2/day2-0200 h	Small	54	14.316	13.9	0.416	0.9167
Subject C/CR2/day1-1600 h	Subject C/CR2/day2-0400 h	Small	53	16.316	17	0.684	0.7862
Subject C/CR2/day1-1800 h	Subject C/CR2/day2-0600 h	Small	53	18.316	17.7	0.616	0.7891
Subject C/CR2/day1-2000 h	Subject C/CR2/day2-0800 h	Small	53	20.316	19.5	0.816	0.7909
Subject C/CR2/day1-2200 h	Subject C/CR2/day2-1000 h	Small	52	22.316	22.1	0.216	0.8398
Subject C/CR2/day2-0000 h	Subject C/CR2/day2-1200 h	Small	40	0.316	0.9	0.584	0.8237
Subject C/CR2/day2-0200 h	Subject C/CR2/day2-1400 h	Small	55	2.316	1.6	0.716	0.9187

Table S1. Cont.

Target sample	Antiphasic sample	Shift group	Used peaks	Expected phase	Estimated phase	Difference	Correlation
Subject C/CR2/day2-0400 h	Subject C/CR2/day2-1600 h	Small	54	4.316	4.6	0.284	0.767
Subject C/CR2/day2-0600 h	Subject C/CR2/day2-1800 h	Small	54	6.316	4.8	1.516	0.6854
Subject C/CR2/day2-0800 h	Subject C/CR2/day2-2000 h	Small	55	8.316	7	1.316	0.5188
Subject D/CR2/day1-1200 h	Subject D/CR2/day2-0000 h	Moderate	54	9.5643	10.1	0.5357	0.8122
Subject D/CR2/day1-1400 h	Subject D/CR2/day2-0200 h	Moderate	51	11.5643	12.8	1.2357	0.8719
Subject D/CR2/day1-1600 h	Subject D/CR2/day2-0400 h	Moderate	50	13.5643	14.4	0.8357	0.9339
Subject D/CR2/day1-1800 h	Subject D/CR2/day2-0600 h	Moderate	54	15.5643	17	1.4357	0.8806
Subject D/CR2/day1-2000 h	Subject D/CR2/day2-0800 h	Moderate	55	17.5643	18.9	1.3357	0.9025
Subject D/CR2/day1-2200 h	Subject D/CR2/day2-1000 h	Moderate	51	19.5643	18.5	1.0643	0.8251
Subject D/CR2/day2-0000 h	Subject D/CR2/day2-1200 h	Moderate	52	21.5643	21.9	0.3357	0.8281
Subject D/CR2/day2-0200 h	Subject D/CR2/day2-1400 h	Moderate	53	23.5643	23.8	0.2357	0.8928
Subject D/CR2/day2-0400 h	Subject D/CR2/day2-1600 h	Moderate	54	1.5643	0.5	1.0643	0.9008
Subject D/CR2/day2-0600 h	Subject D/CR2/day2-1800 h	Moderate	54	3.5643	4	0.4357	0.9171
Subject D/CR2/day2-0800 h	Subject D/CR2/day2-2000 h	Moderate	53	5.5643	8	2.4357	0.7937
Subject E/CR2/day1-1200 h	Subject E/CR2/day2-0000 h	Large	32	1.8748	4.6	2.7252	0.6901
Subject E/CR2/day1-1400 h	Subject E/CR2/day2-0200 h	Large	36	3.8748	6.5	2.6252	0.5885
Subject E/CR2/day1-1600 h	Subject E/CR2/day2-0400 h	Large	36	5.8748	7.2	1.3252	0.7302
Subject E/CR2/day1-1800 h	Subject E/CR2/day2-0600 h	Large	37	7.8748	10.4	2.5252	0.8376
Subject E/CR2/day1-2000 h	Subject E/CR2/day2-0800 h	Large	40	9.8748	12.1	2.2252	0.7948
Subject E/CR2/day1-2200 h	Subject E/CR2/day2-1000 h	Large	34	11.8748	14	2.1252	0.8367
Subject E/CR2/day2-0000 h	Subject E/CR2/day2-1200 h	Large	25	13.8748	17.1	3.2252	0.6317
Subject E/CR2/day2-0200 h	Subject E/CR2/day2-1400 h	Large	34	15.8748	17.5	1.6252	0.8155
Subject E/CR2/day2-0400 h	Subject E/CR2/day2-1600 h	Large	31	17.8748	18.2	0.3252	0.7895
Subject E/CR2/day2-0600 h	Subject E/CR2/day2-1800 h	Large	37	19.8748	21.4	1.5252	0.7689
Subject E/CR2/day2-0800 h	Subject E/CR2/day2-2000 h	Large	42	21.8748	22.6	0.7252	0.8389
Subject F/CR2/day1-1200 h	Subject F/CR2/day2-0000 h	Moderate	53	8.1484	8.6	0.4516	0.6177
Subject F/CR2/day1-1400 h	Subject F/CR2/day2-0200 h	Moderate	49	10.1484	9.8	0.3484	0.7872
Subject F/CR2/day1-1600 h	Subject F/CR2/day2-0400 h	Moderate	51	12.1484	11.8	0.3484	0.9449
Subject F/CR2/day1-1800 h	Subject F/CR2/day2-0600 h	Moderate	50	14.1484	14	0.1484	0.938
Subject F/CR2/day1-2000 h	Subject F/CR2/day2-0800 h	Moderate	47	16.1484	16.7	0.5516	0.895
Subject F/CR2/day1-2200 h	Subject F/CR2/day2-1000 h	Moderate	47	18.1484	15.4	2.7484	0.8886
Subject F/CR2/day2-0000 h	Subject F/CR2/day2-1200 h	Moderate	48	20.1484	18.6	1.5484	0.806
Subject F/CR2/day2-0200 h	Subject F/CR2/day2-1400 h	Moderate	49	22.1484	20.5	1.6484	0.7134
Subject F/CR2/day2-0400 h	Subject F/CR2/day2-1600 h	Moderate	52	0.1484	23.1	1.0484	0.8966
Subject F/CR2/day2-0600 h	Subject F/CR2/day2-1800 h	Moderate	51	2.1484	0.3	1.8484	0.9222
Subject F/CR2/day2-0800 h	Subject F/CR2/day2-2000 h	Moderate	50	4.1484	3.8	0.3484	0.8857

The format of the blood samples is subject name/condition (CR1 or CR2)/day (1 or 2)-time of day (0000–2200 h).

Fig. S1. Procedure to select metabolite peaks for our human metabolic molecular timetable construction.

Fig. S1

Fig. S2. Estimation of human body time. (*A*) Correlation between cortisol peak time and melatonin peak time. Expected body time is calculated by conventional method using cortisol time-course abundance in this study. Expected body time calculated by melatonin time-course abundance also provides a similar expected body time because there is strong correlation between cortisol and melatonin peak times. (*B*) Summary of expected body time and estimated body time. *X* axes show sampling time (h) and *y* axes show estimated or expected body time (h). Red dot indicates estimated body time; blue and black dashed lines indicate expected body time and sampled time, respectively. Expected body time (based on cortisol rhythm) and estimated body time (based on molecular timetable) were similar in all samples, which is indicated by the observation that the red dots are near blue dashed lines. (*C*) Details of body-time estimation results. Results of all body-time estimation performed in this study are shown. Colors of the dots indicate the molecular peak times of each metabolite. Peak time of the red cosine curves indicates estimated body time; peak time of the blue cosine curves indicates expected body time. Dashed vertical lines show the estimated body time (red) or expected body time (blue). Header of each graph indicates the blood sample in the format subject name/condition (CR1 or CR2)/day (1 or 2)-time (0000–2200 h).

Fig. S2

Fig. S3. Identified circadian-oscillating metabolites. (*A*–*D*) Abundance is shown of pregnenolone 3-sulfate (*A*), dehydroepiandrosterone sulfate (*B*), PG(18:1(9Z)/0:0) (*C*), and LysoPC(16:0) (*D*) in the blood taken from three subjects (subjects A–C). *X* axes show the sampled time (h); *y* axes show normalized area of the corresponding peak in LC–MS analysis. We note that pregnenolone 3-sulfate in Fig. S3*A* and pregnanolone sulfate-like metabolite are different metabolites. (*E*) Identified circadian-oscillating metabolites in the steroid hormone pathway. Identified circadian-oscillating metabolites are indicated in red letters and arrows. Numbers in parentheses show the peak time of each metabolite.

Fig. S3

Fig. S4. Evaluation of methods for the timetable construction and body-time estimation. (*A* and *B*) Evaluation of body-time estimation based on dim-light melatonin onset (DLMO). (*A*) Difference between the expected body time based on DLMO and the sampled time. Nine sample sets for body-time estimation were classified into three groups by the magnitude of the difference: small (black), moderate (gray), and large (white). (*B*) Summary of body-time estimation. Difference between expected and estimated body time for all estimated samples is shown, in which expected body time was determined on the basis of DLMO, as shown in Fig. 3*E*. (*C*) Evaluation of body-time estimation using a single time point and three time points separated by 8 h. *X* axis shows the number of time points used in the body-time estimation and the *y* axis shows the time difference. Each whisker represents the range of time differences; each red box represents the range of 0.25 and 0.75 quartiles of the time differences, and the horizontal line in each red box is the median of the time differences. (*D*) Bias in selection of subjects for the molecular timetable construction. The *x* axis shows the combination of subjects whose samples were used in the timetable construction and the *y* axis shows the time difference as shown in *C*.

Fig. S4

Dataset S1. List of identified circadian-oscillating metabolites

Dataset S1

The list contains two sheets, one for a list of circadian-oscillating metabolite detected in the positive-ion mode, and the other is in the negative-ion mode. Each sheet lists the unique number, *m/z*, retention time (RT), a mark (*) whether the metabolite is used in the human blood metabolite timetable, the name of the metabolite if experimentally identified, the names of computationally predicted metabolites, mean of peak areas, SD of peak areas, peak time (phase), maximum correlation to cosine curves, *P* value of the cosine fitting, FDR of the cosine fitting, *P* value of the ANOVA test, FDR of the ANOVA test, and peak areas for all blood samples.

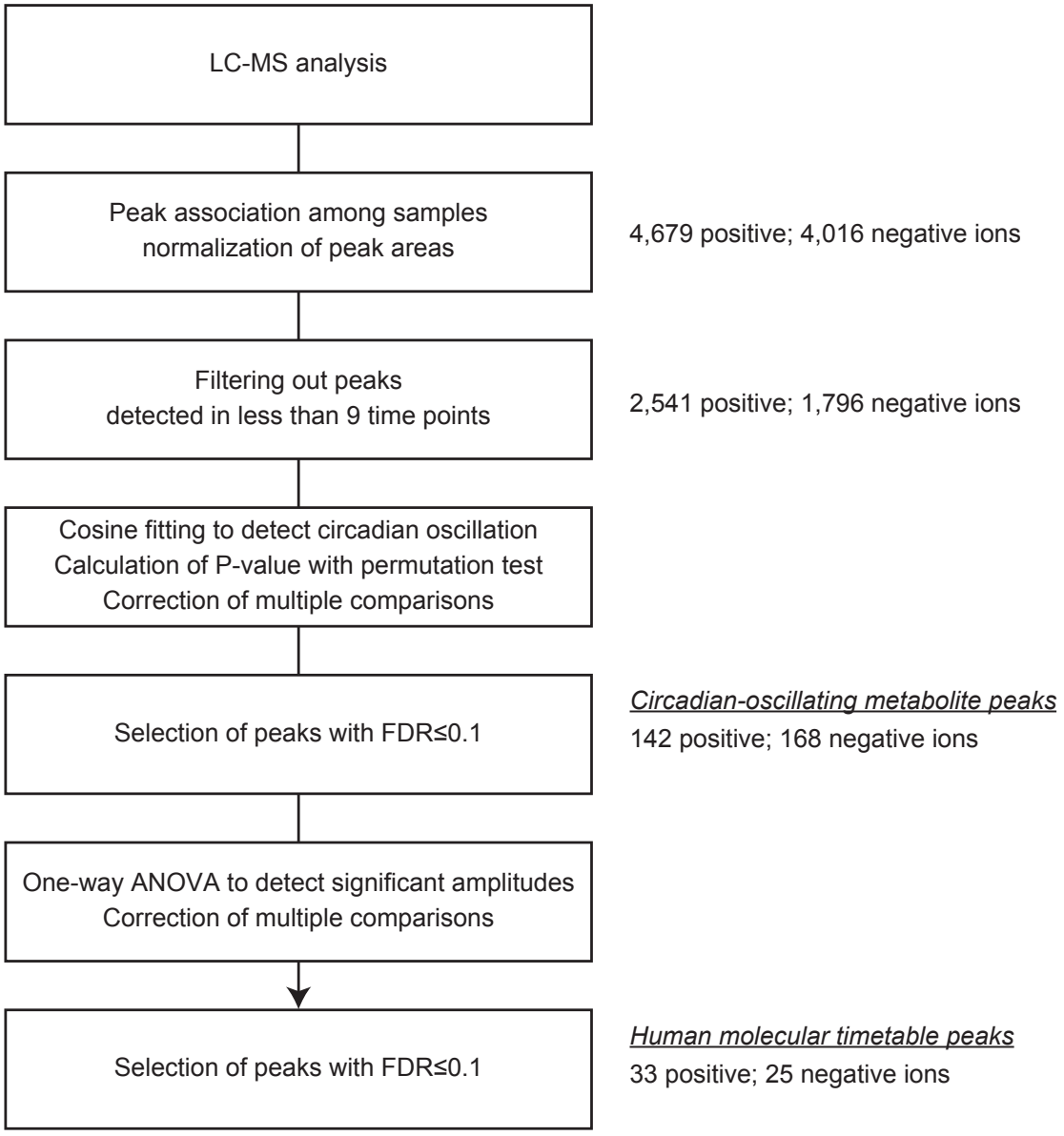
LC-MS analysis
Peak association among samples
normalization of peak areas
4,679 positive; 4,016 negative ions
Filtering out peaks
detected in less than 9 time points
2,541 positive; 1,796 negative ions
Cosine fitting to detect circadian oscillation
Calculation of P-value with permutation test
Correction of multiple comparisons
Selection of peaks with FDR≤0.1
Circadian-oscillating metabolite peaks
142 positive; 168 negative ions
One-way ANOVA to detect significant amplitudes
Correction of multiple comparisons
Selection of peaks with FDR≤0.1
Human molecular timetable peaks
33 positive; 25 negative ions

Fig. S1

Fig. S2

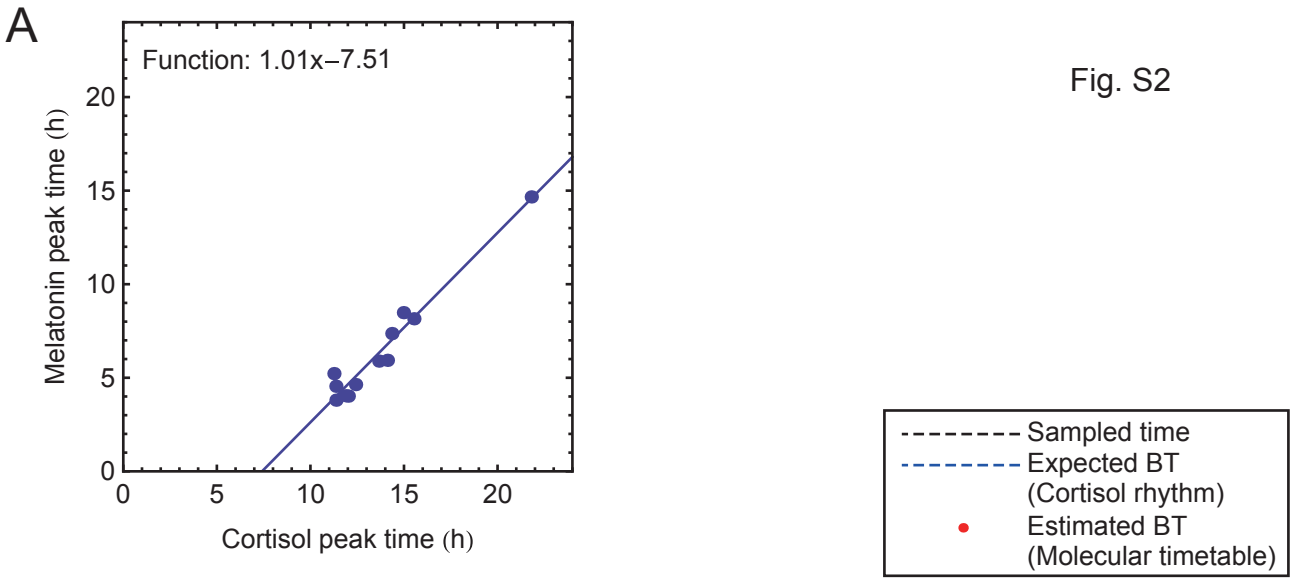
A
Function: 1.01x–7.51
Melatonin peak time (h)
Cortisol peak time (h)
Sampled time
Expected BT
(Cortisol rhythm)
Estimated BT
(Molecular timetable)

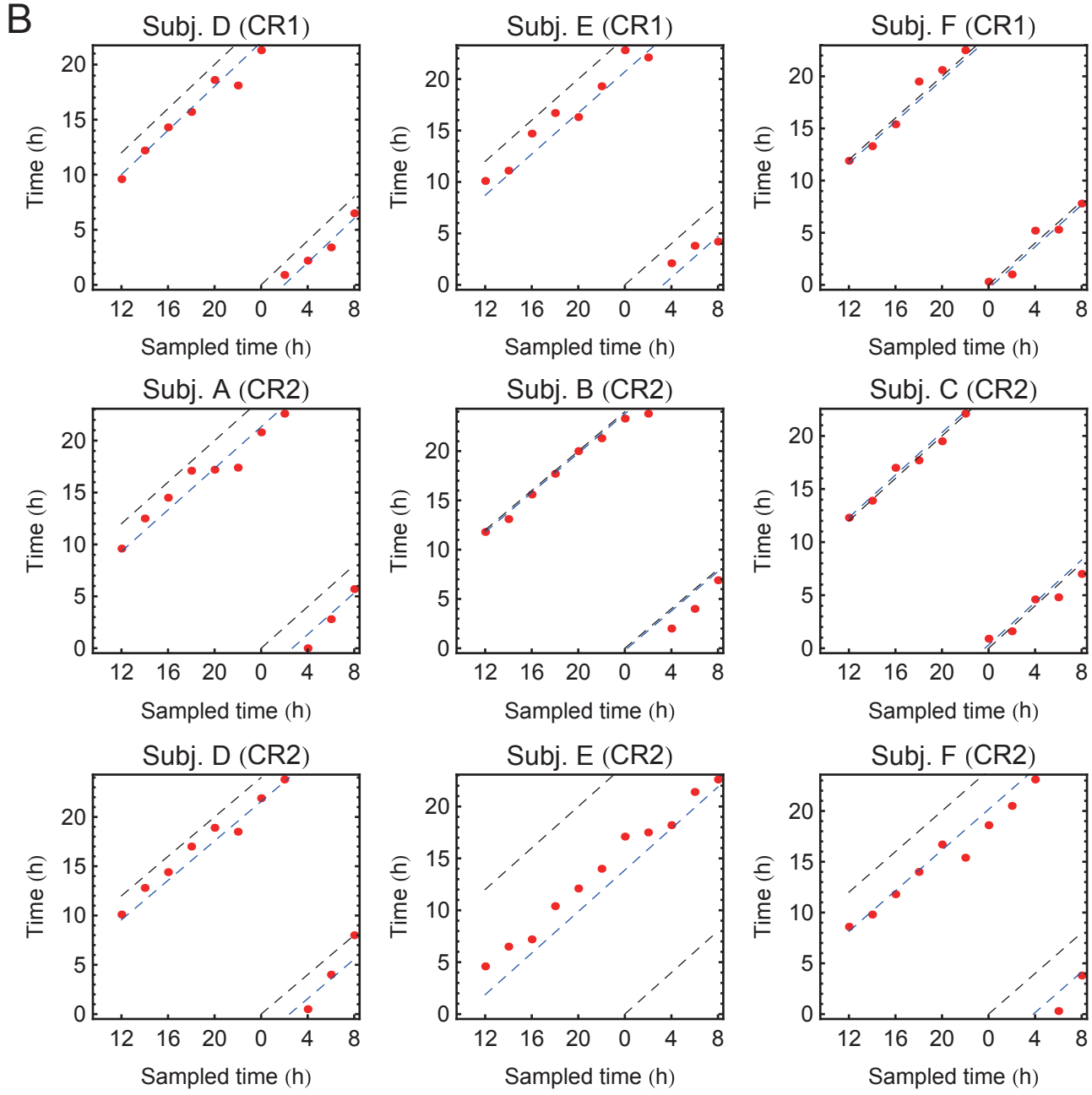
B
Subj. D (CR1)
Subj. E (CR1)
Subj. F (CR1)
Subj. A (CR2)
Subj. B (CR2)
Subj. C (CR2)
Subj. D (CR2)
Subj. E (CR2)
Subj. F (CR2)
Time (h)
Sampled time (h)

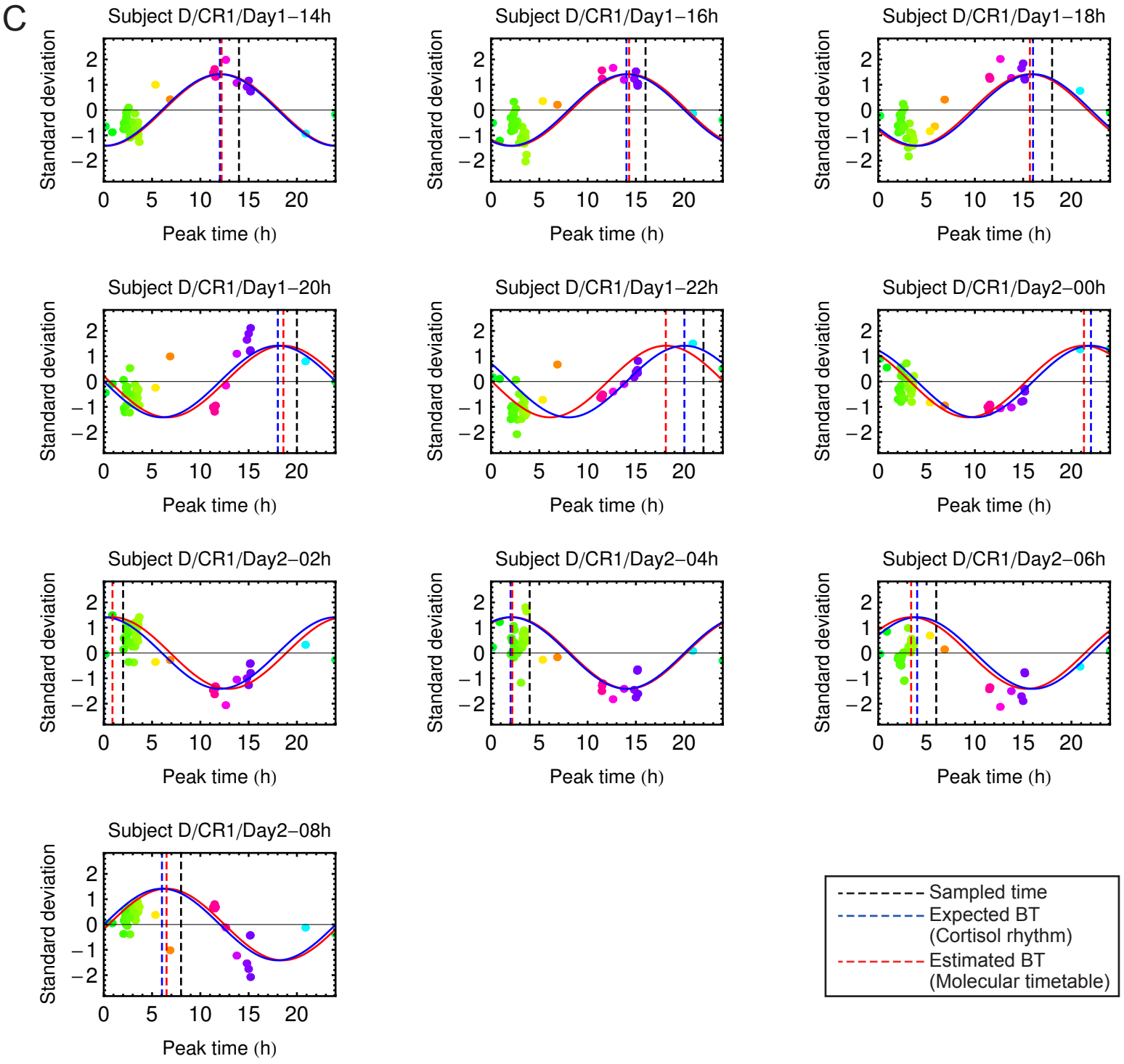
C
Subject D/CR1/Day1−14h
Subject D/CR1/Day1−16h
Subject D/CR1/Day1−18h
Subject D/CR1/Day1−20h
Subject D/CR1/Day1−22h
Subject D/CR1/Day2−00h
Subject D/CR1/Day2−02h
Subject D/CR1/Day2−04h
Subject D/CR1/Day2−06h
Subject D/CR1/Day2−08h
Standard deviation
Peak time (h)
Sampled time
Expected BT
(Cortisol rhythm)
Estimated BT
(Molecular timetable)

Fig. S2

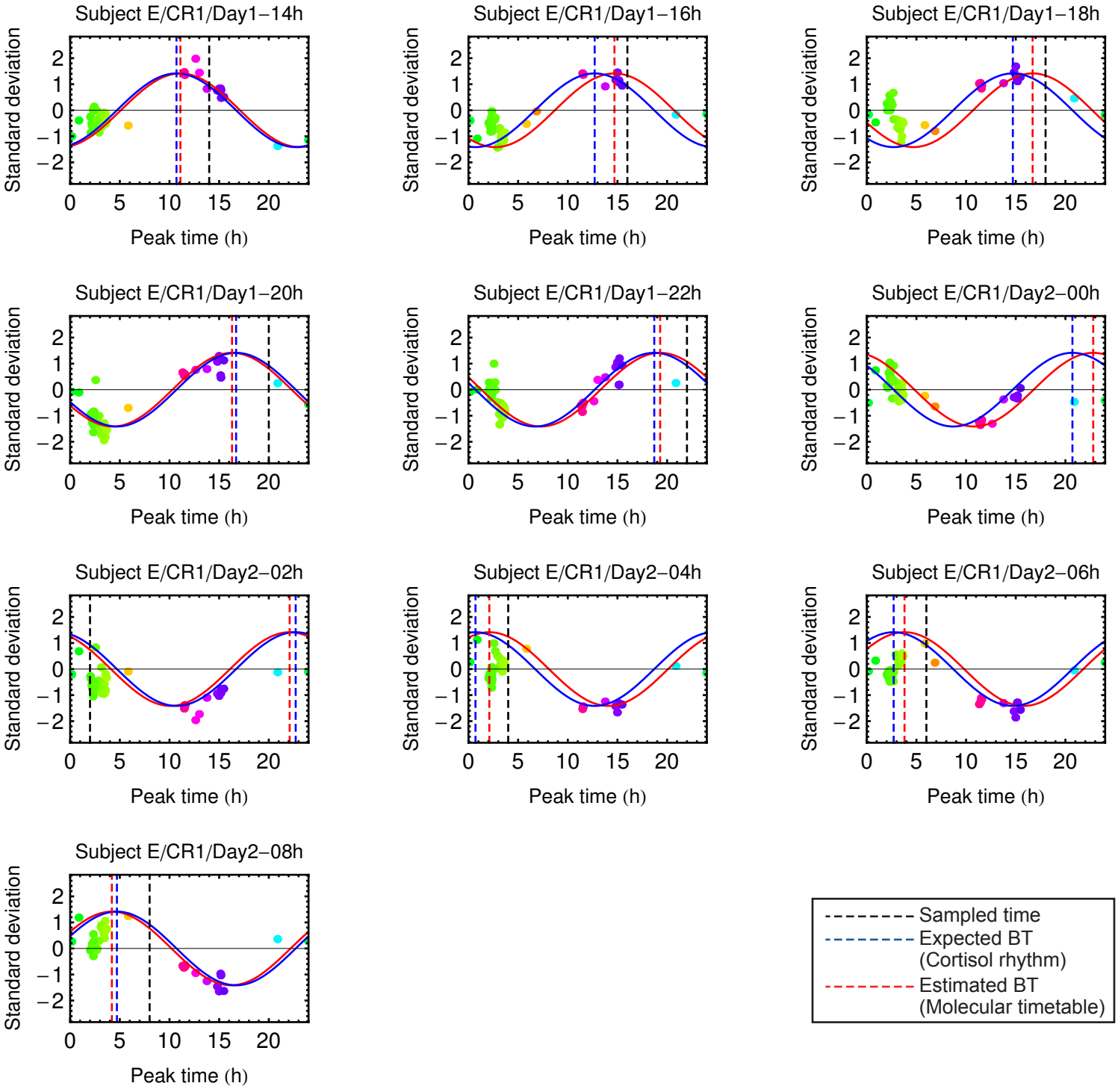
Subject E/CR1/Day1−14h
Subject E/CR1/Day1−16h
Subject E/CR1/Day1−18h
Subject E/CR1/Day1−20h
Subject E/CR1/Day1−22h
Subject E/CR1/Day2−00h
Subject E/CR1/Day2−02h
Subject E/CR1/Day2−04h
Subject E/CR1/Day2−06h
Subject E/CR1/Day2−08h
Standard deviation
Peak time (h)
Sampled time
Expected BT
(Cortisol rhythm)
Estimated BT
(Molecular timetable)

Fig. S2

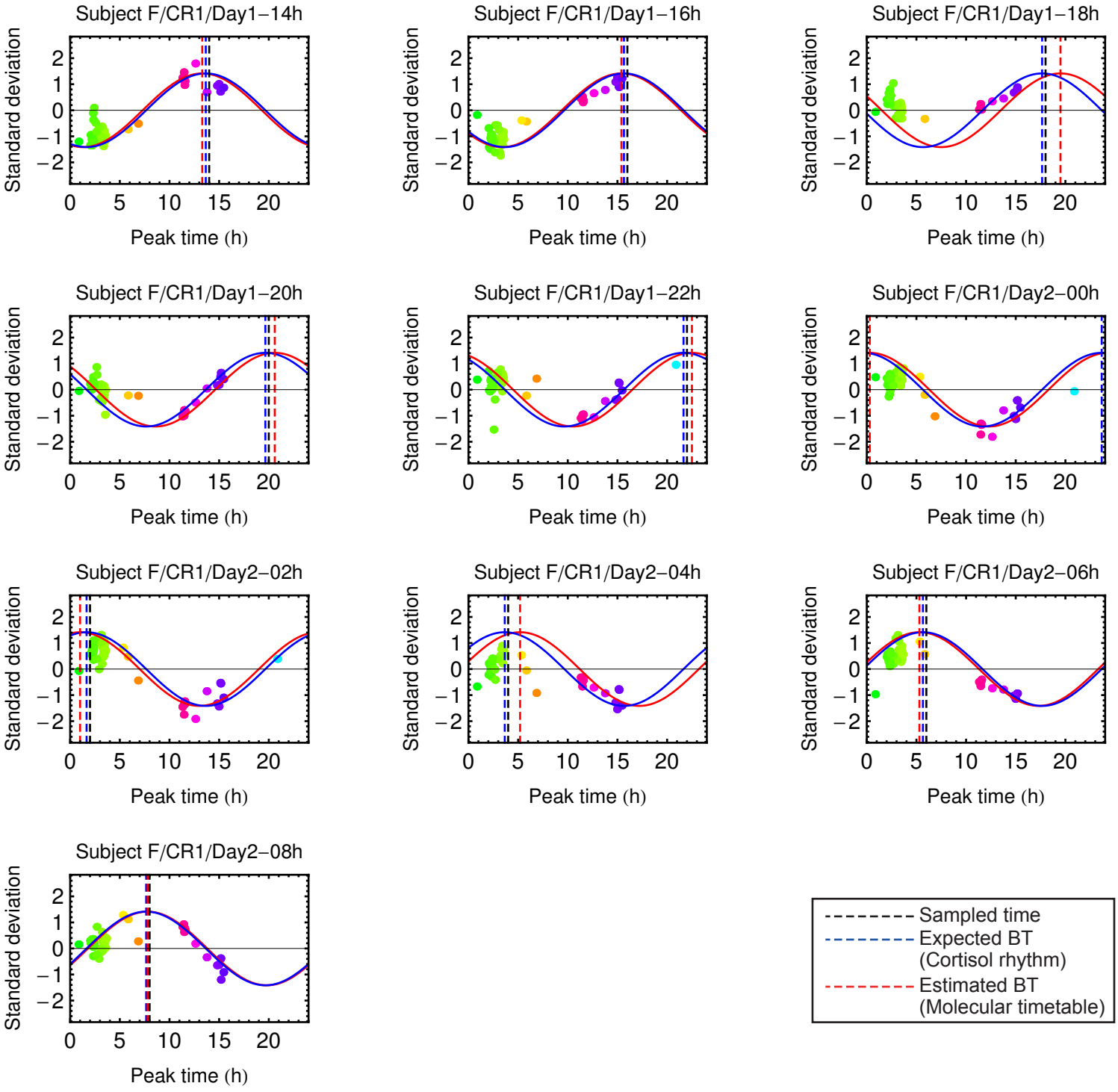
Subject F/CR1/Day1−14h
Subject F/CR1/Day1−16h
Subject F/CR1/Day1−18h
Subject F/CR1/Day1−20h
Subject F/CR1/Day1−22h
Subject F/CR1/Day2−00h
Subject F/CR1/Day2−02h
Subject F/CR1/Day2−04h
Subject F/CR1/Day2−06h
Subject F/CR1/Day2−08h
Standard deviation
Peak time (h)
Sampled time
Expected BT
(Cortisol rhythm)
Estimated BT
(Molecular timetable)

Fig. S2

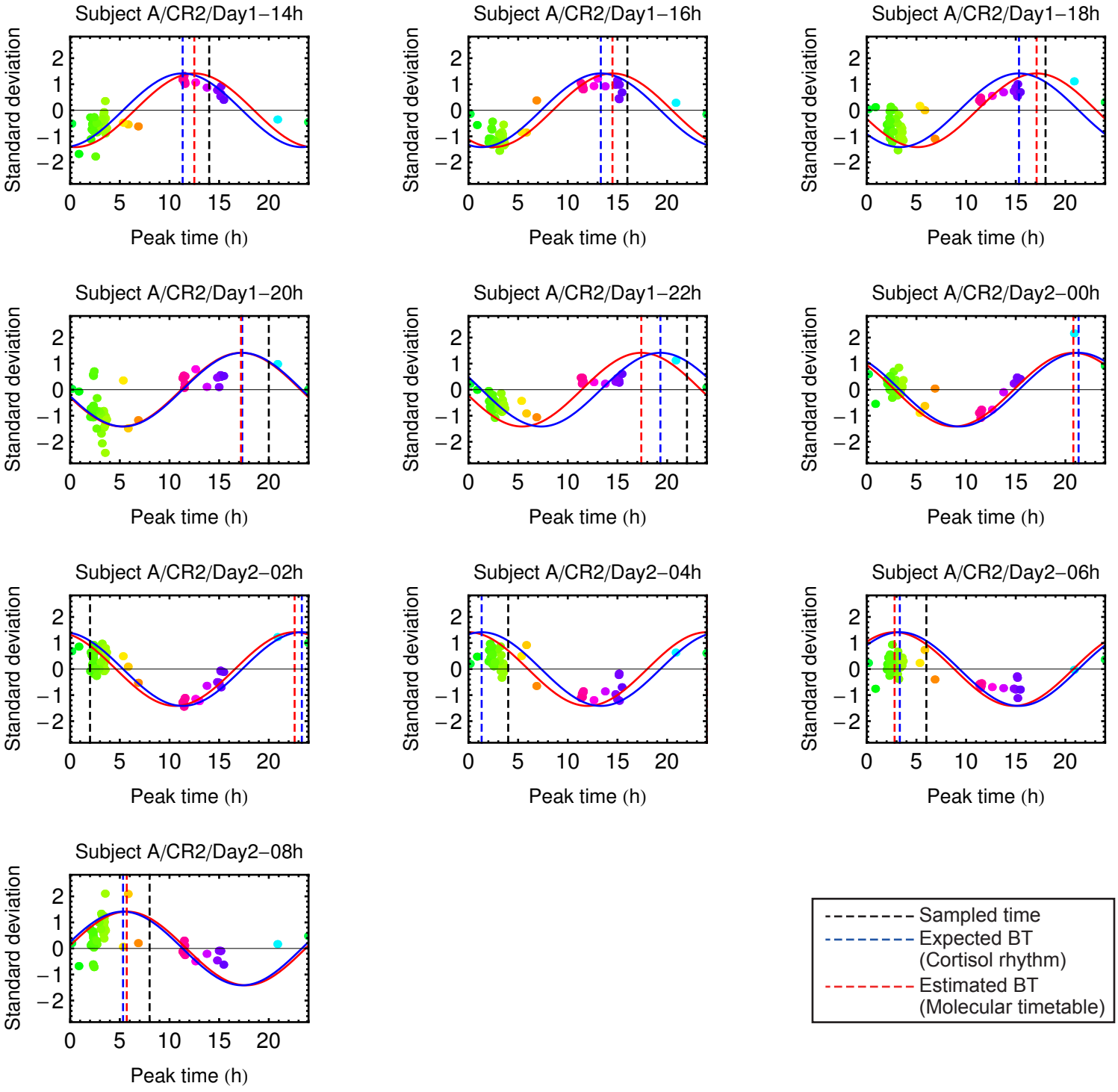
Subject A/CR2/Day1−14h
Subject A/CR2/Day1−16h
Subject A/CR2/Day1−18h
Subject A/CR2/Day1−20h
Subject A/CR2/Day1−22h
Subject A/CR2/Day2−00h
Subject A/CR2/Day2−02h
Subject A/CR2/Day2−04h
Subject A/CR2/Day2−06h
Subject A/CR2/Day2−08h
Standard deviation
Peak time (h)
Sampled time
Expected BT
(Cortisol rhythm)
Estimated BT
(Molecular timetable)

Fig. S2

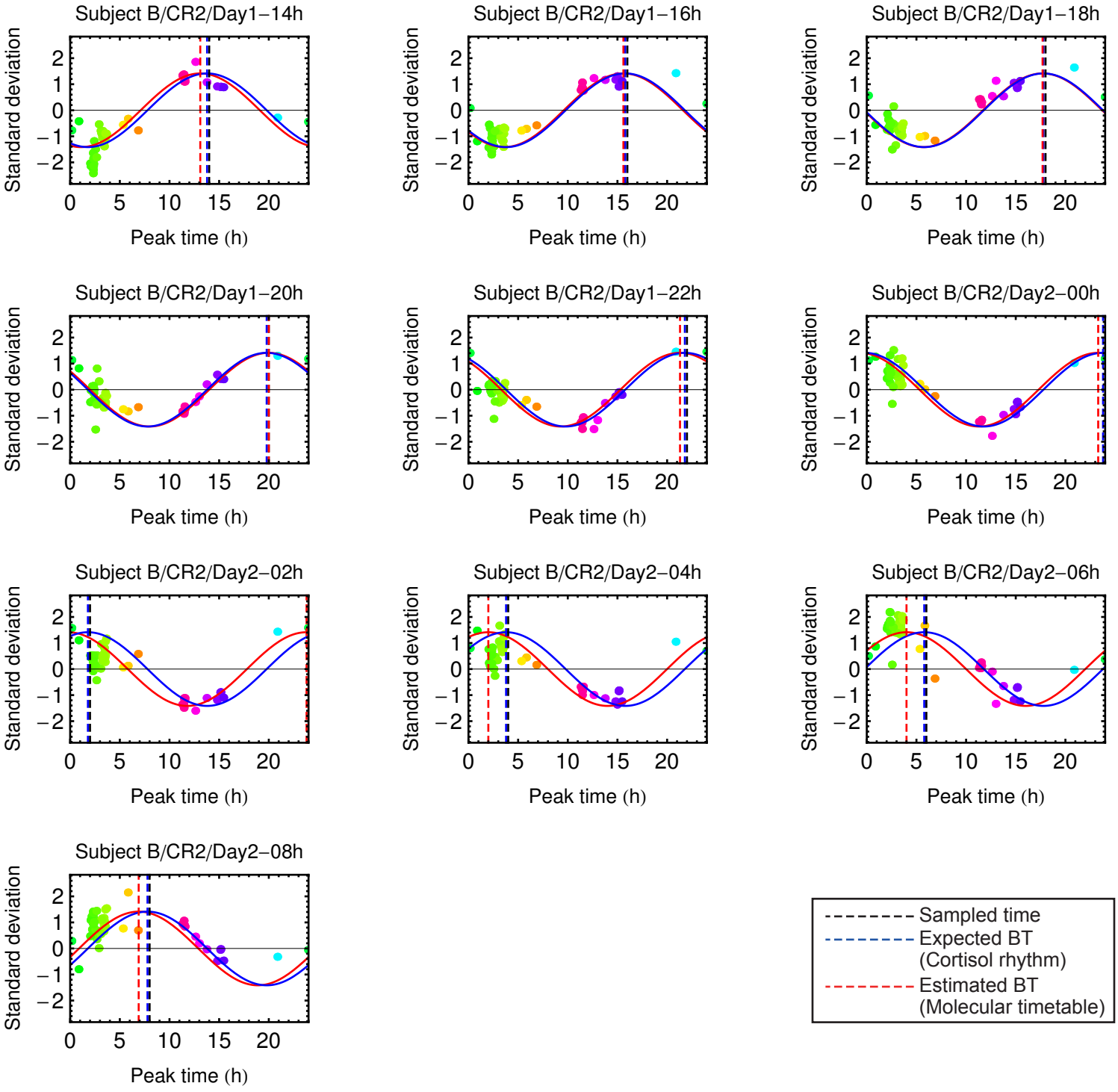
Subject B/CR2/Day1−14h
Subject B/CR2/Day1−16h
Subject B/CR2/Day1−18h
Subject B/CR2/Day1−20h
Subject B/CR2/Day1−22h
Subject B/CR2/Day2−00h
Subject B/CR2/Day2−02h
Subject B/CR2/Day2−04h
Subject B/CR2/Day2−06h
Subject B/CR2/Day2−08h
Standard deviation
Peak time (h)
Sampled time
Expected BT
(Cortisol rhythm)
Estimated BT
(Molecular timetable)

Fig. S2

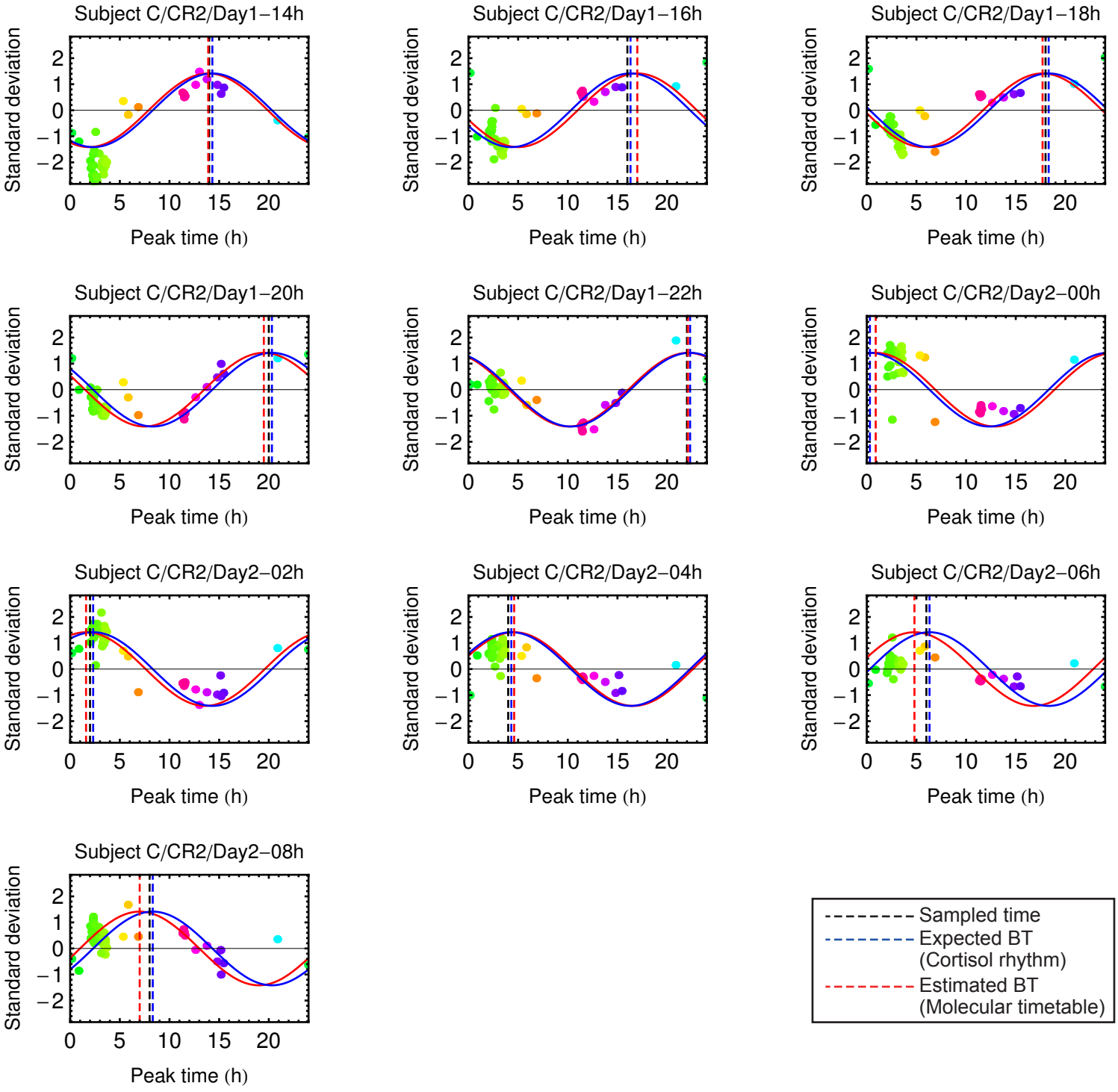
Subject C/CR2/Day1−14h
Subject C/CR2/Day1−16h
Subject C/CR2/Day1−18h
Subject C/CR2/Day1−20h
Subject C/CR2/Day1−22h
Subject C/CR2/Day2−00h
Subject C/CR2/Day2−02h
Subject C/CR2/Day2−04h
Subject C/CR2/Day2−06h
Subject C/CR2/Day2−08h
Standard deviation
Peak time (h)
Sampled time
Expected BT
(Cortisol rhythm)
Estimated BT
(Molecular timetable)

Fig. S2

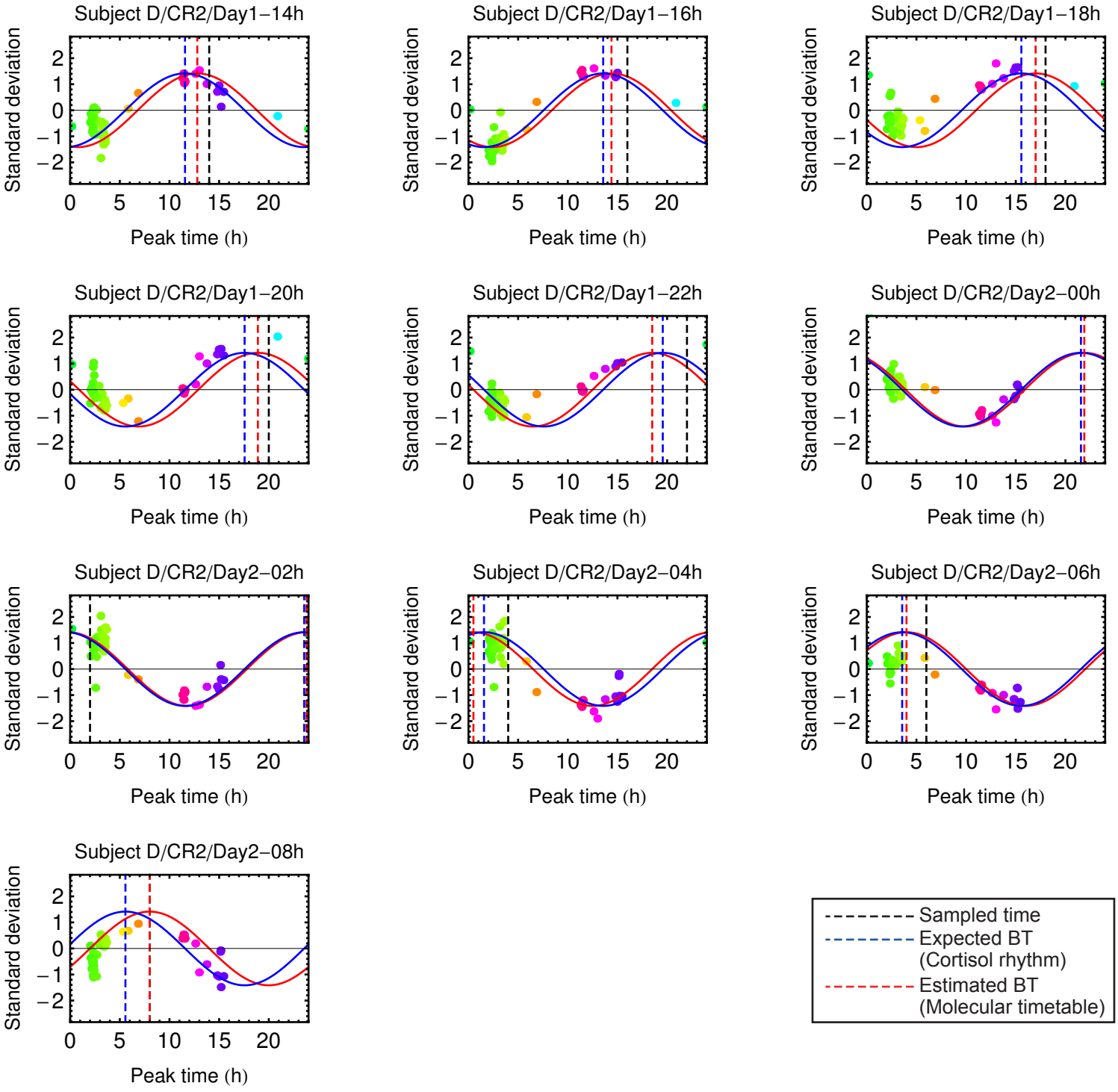
Subject D/CR2/Day1−14h
Subject D/CR2/Day1−16h
Subject D/CR2/Day1−18h
Subject D/CR2/Day1−20h
Subject D/CR2/Day1−22h
Subject D/CR2/Day2−00h
Subject D/CR2/Day2−02h
Subject D/CR2/Day2−04h
Subject D/CR2/Day2−06h
Subject D/CR2/Day2−08h
Standard deviation
Peak time (h)
Sampled time
Expected BT
(Cortisol rhythm)
Estimated BT
(Molecular timetable)

Fig. S2

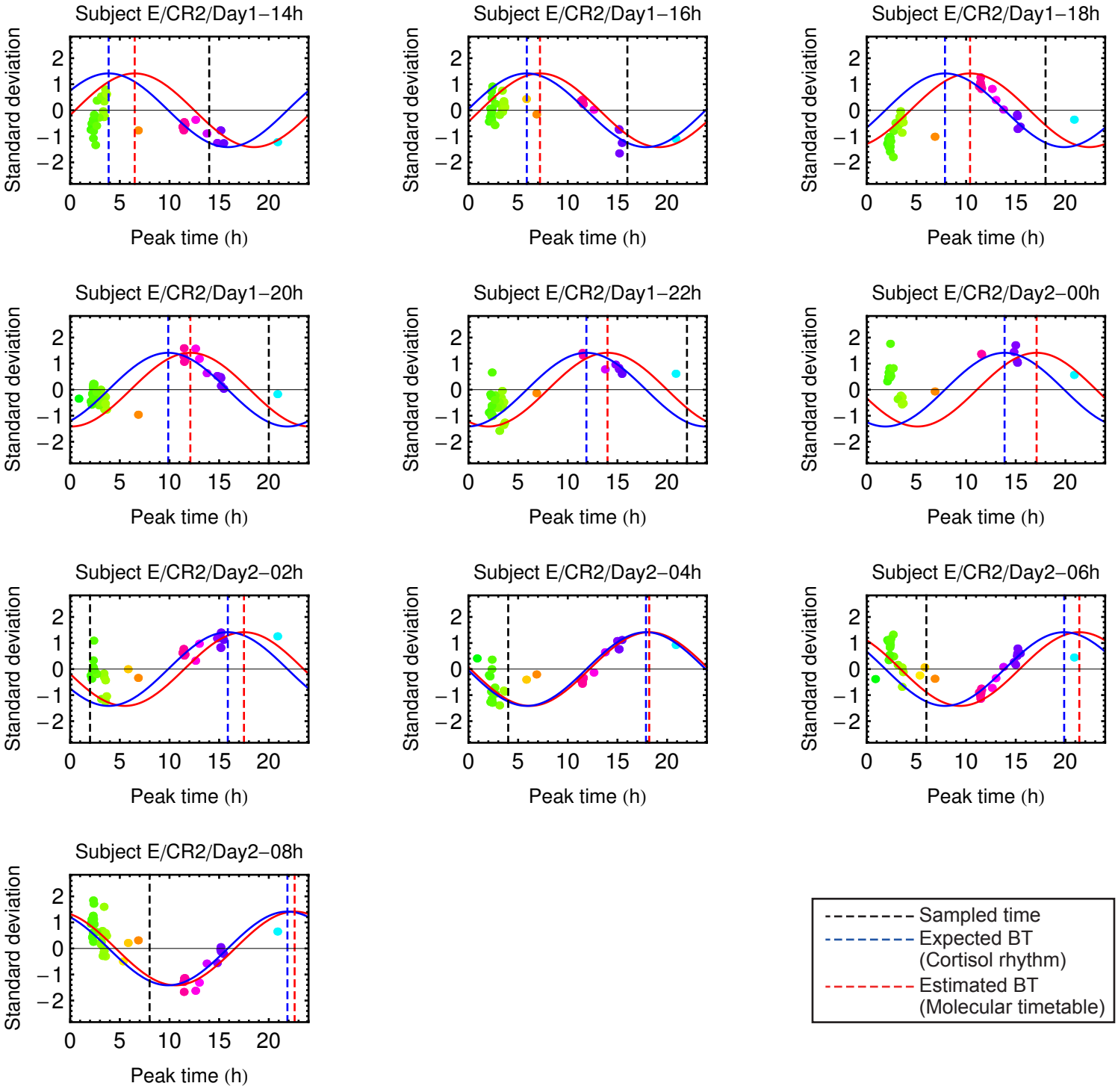
Subject E/CR2/Day1−14h
Subject E/CR2/Day1−16h
Subject E/CR2/Day1−18h
Subject E/CR2/Day1−20h
Subject E/CR2/Day1−22h
Subject E/CR2/Day2−00h
Subject E/CR2/Day2−02h
Subject E/CR2/Day2−04h
Subject E/CR2/Day2−06h
Subject E/CR2/Day2−08h
Standard deviation
Peak time (h)
Sampled time
Expected BT
(Cortisol rhythm)
Estimated BT
(Molecular timetable)

Fig. S2

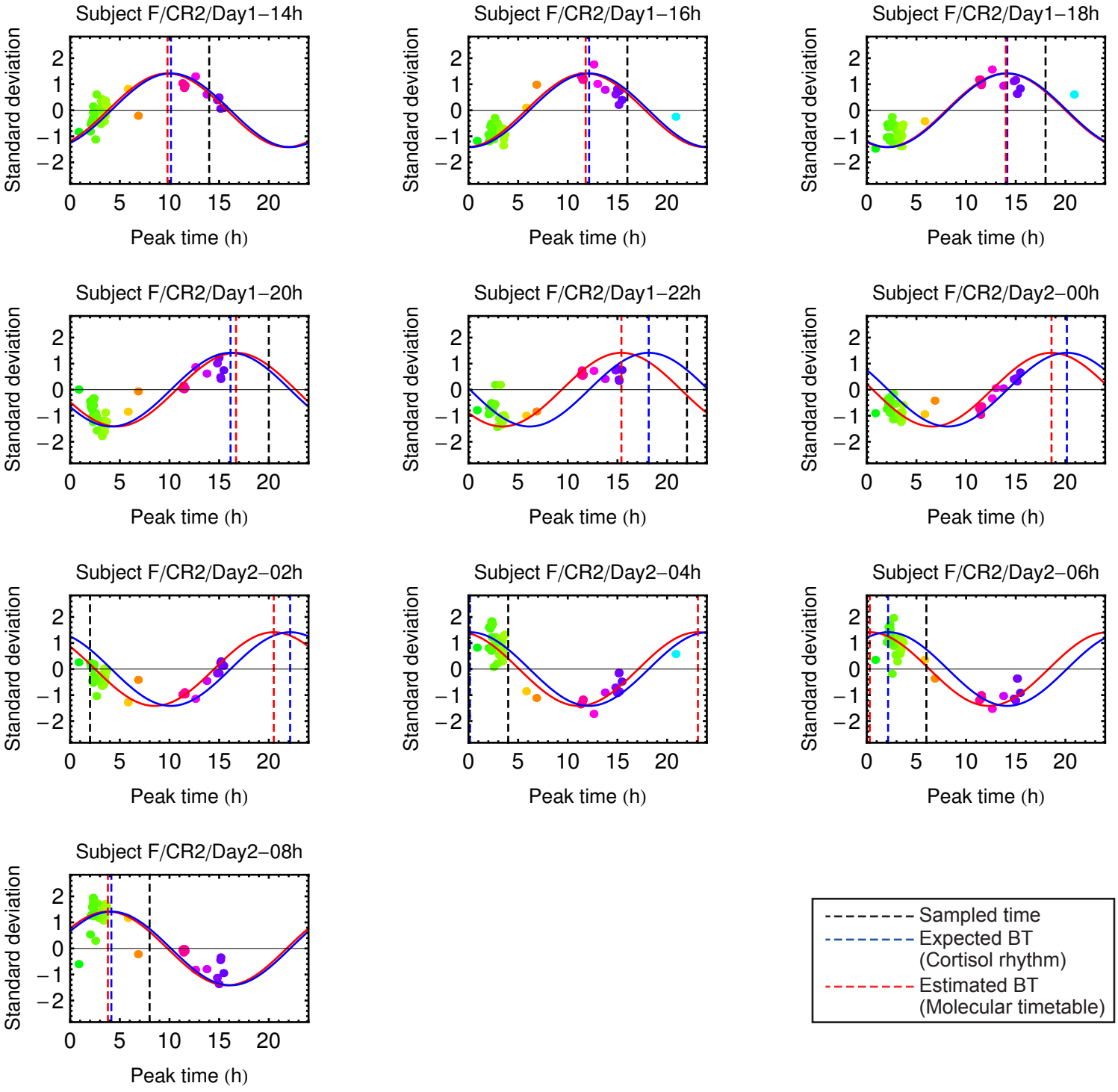
Subject F/CR2/Day1−14h
Subject F/CR2/Day1−16h
Subject F/CR2/Day1−18h
Subject F/CR2/Day1−20h
Subject F/CR2/Day1−22h
Subject F/CR2/Day2−00h
Subject F/CR2/Day2−02h
Subject F/CR2/Day2−04h
Subject F/CR2/Day2−06h
Subject F/CR2/Day2−08h
Standard deviation
Peak time (h)
Sampled time
Expected BT
(Cortisol rhythm)
Estimated BT
(Molecular timetable)

Fig. S2

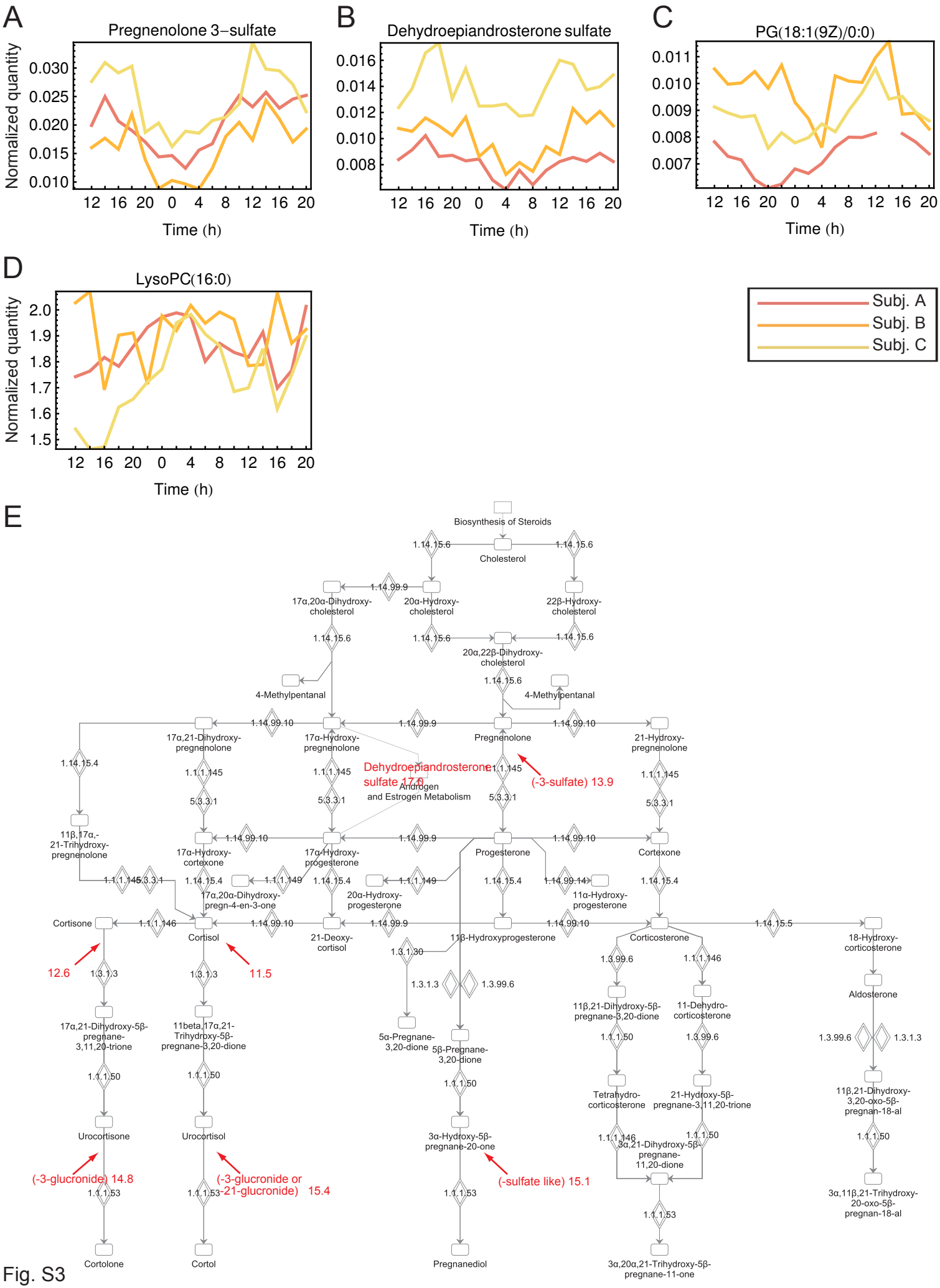
A
Pregnenolone 3−sulfate
Normalized quantity
0.030
0.025
0.020
0.015
0.010
12 16 20 0 4 8 12 16 20
Time (h)
B
Dehydroepiandrosterone sulfate
0.016
0.014
0.012
0.010
0.008
12 16 20 0 4 8 12 16 20
Time (h)
C
PG(18:1(9Z)/0:0)
0.011
0.010
0.009
0.008
0.007
12 16 20 0 4 8 12 16 20
Time (h)
D
LysoPC(16:0)
Normalized quantity
2.0
1.9
1.8
1.7
1.6
1.5
12 16 20 0 4 8 12 16 20
Time (h)
Subj. A
Subj. B
Subj. C
E
Biosynthesis of Steroids
Cholesterol
17α,20α-Dihydroxy-cholesterol
20α-Hydroxy-cholesterol
22β-Hydroxy-cholesterol
20α,22β-Dihydroxy-cholesterol
4-Methylpentanal
17α,21-Dihydroxy-pregnenolone
17α-Hydroxy-pregnenolone
Pregnenolone
21-Hydroxy-pregnenolone
Androgen and Estrogen Metabolism
Dehydroepiandrosterone sulfate 17.0
(-3-sulfate) 13.9
11β,17α,-21-Trihydroxy-pregnenolone
17α-Hydroxy-cortexone
17α-Hydroxy-progesterone
Progesterone
Cortexone
17α,20α-Dihydroxy-pregn-4-en-3-one
20α-Hydroxy-progesterone
11α-Hydroxy-progesterone
Cortisone
Cortisol
21-Deoxy-cortisol
11β-Hydroxyprogesterone
Corticosterone
18-Hydroxy-corticosterone
12.6
11.5
17α,21-Dihydroxy-5β-pregnane-3,11,20-trione
11beta,17α,21-Trihydroxy-5β-pregnane-3,20-dione
5α-Pregnane-3,20-dione
5β-Pregnane-3,20-dione
11β,21-Dihydroxy-5β-pregnane-3,20-dione
11-Dehydro-corticosterone
Aldosterone
Urocortisone
Urocortisol
3α-Hydroxy-5β-pregnane-20-one
Tetrahydro-corticosterone
21-Hydroxy-5β-pregnane-3,11,20-trione
11β,21-Dihydroxy-3,20-oxo-5β-pregnan-18-al
(-3-glucronide) 14.8
(-3-glucronide or 21-glucronide) 15.4
(-sulfate like) 15.1
3α,21-Dihydroxy-5β-pregnane-11,20-dione
3α,11β,21-Trihydroxy-20-oxo-5β-pregnan-18-al
Cortolone
Cortol
Pregnanediol
3α,20α,21-Trihydroxy-5β-pregnane-11-one

Fig. S3

Fig. S4

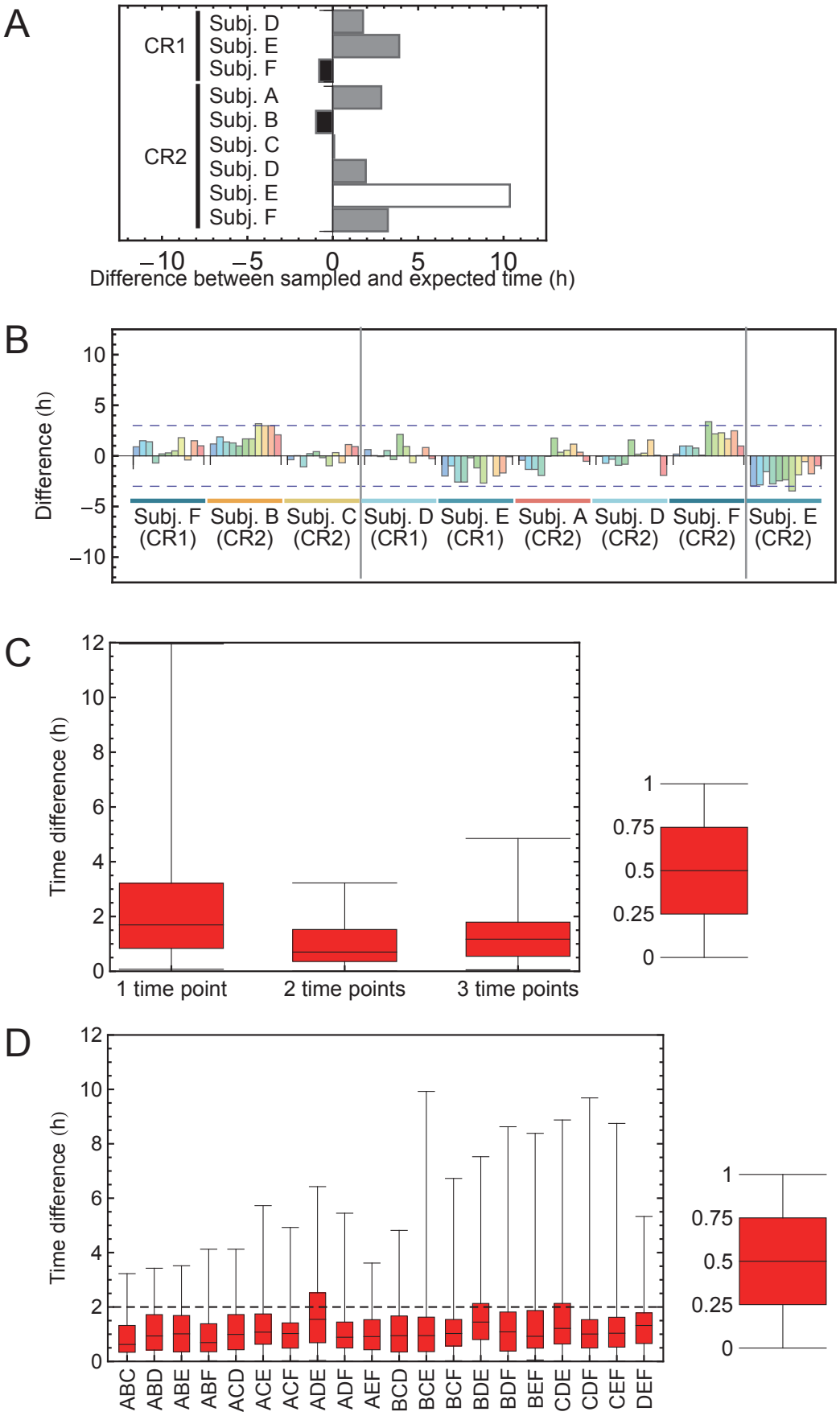
A
CR1
Subj. D
Subj. E
Subj. F
CR2
Subj. A
Subj. B
Subj. C
Subj. D
Subj. E
Subj. F
−10
−5
0
5
10
Difference between sampled and expected time (h)
B
Difference (h)
10
5
0
−5
−10
Subj. F (CR1)
Subj. B (CR2)
Subj. C (CR2)
Subj. D (CR1)
Subj. E (CR1)
Subj. A (CR2)
Subj. D (CR2)
Subj. F (CR2)
Subj. E (CR2)
C
Time difference (h)
12
10
8
6
4
2
0
1 time point
2 time points
3 time points
1
0.75
0.5
0.25
0
D
Time difference (h)
12
10
8
6
4
2
0
ABC
ABD
ABE
ABF
ACD
ACE
ACF
ADE
ADF
AEF
BCD
BCE
BCF
BDE
BDF
BEF
CDE
CDF
CEF
DEF
1
0.75
0.5
0.25
0